NATIONAL AND KAPODISTRIAN UNIVERSITY OF ATHENS

SCHOOL OF MEDICINE

POSTGRADUATE PROGRAM

“MEDICAL AND SURGICAL RETINA MODERN APPROACHES”

DIRECTOR: PROFESSOR I. GEORGALAS

POSTGRADUATE THESIS

Artificial Intelligence and Myopic Maculopathy: the Role of Advanced Imaging Techniques in the Diagnosis, Classification and Follow up of Highly Myopic Cases

MARIA-VARVARA KAPETANAKI

ATHENS, MARCH 2025

NATIONAL AND KAPODISTRIAN UNIVERSITY OF ATHENS
SCHOOL OF MEDICINE
POSTGRADUATE PROGRAM
“MEDICAL AND SURGICAL RETINA MODERN APPROACHES”
DIRECTOR: PROFESSOR I. GEORGALAS

POSTGRADUATE THESIS

Artificial Intelligence and Myopic Maculopathy: The Role of Advanced Imaging Techniques in Diagnosis, Classification and Follow-up of Highly Myopic Cases

MARIA VARVARA KAPETANAKI

SUPERVISOR: PROFESSOR ILIAS GEORGALAS

THREE-MEMBER COMMITTEE

ILIAS GEORGALAS
EIRINI MALIAGKANI
STYLIANOS KANDARAKIS

ATHENS, MARCH 2025

Acknowledgements

I would like to express my gratitude to all the determining factors that contributed and guided the preparation and completion of this thesis. Their presence played a crucial role in shaping the result and their loyal support throughout this turbulent journey undoubtedly supplied me with essential commitment and dedication.

The first to whom I must refer are my family members: my mother, Alexandra, and my four sisters, Katerina, Alexia, Valentina and Nadia, who provided me with stable determination, a necessary tool from the beginning to the end of this procedure.

The next people I would like to thank are Professor Ilias Georgalas and Dr Eirini Maliagkani, whose valuable advice and pertinent observations throughout the writing period ensured the efficient conduct of the investigation and facilitated the correct unfolding of this authorship.

Finally, I would like to express my gratitude to all my friends, my old and my current colleagues, whose psychological and emotional encouragement armed me with useful motivation and strength to complete this diploma.

Sayings and quotes:

Wherever the art of medicine is loved, there is also a love for humanity. ~ Hippocrates

If it were not for the great variability among individuals, medicine might as well be a science, not an art. ~ William Osler

Contents

Abstract

Myopic Maculopathy associated with Pathologic Myopia is a major cause of irreversible visual impairment worldwide that is estimated to have a high prevalence/incidence rate in the future. Therefore, the early detection of pathological changes with the assistance of color fundus photography and optical coherence tomography (OCT) Imaging, the accurate diagnosis/classification but also monitoring of the disease progression are of crucial importance as they can lead to better treatment decisions in everyday clinical practice. The recent development of Artificial Intelligence Tools, the advances in Ultra-Widefield Technology and the optimization of OCT Imaging Techniques have laid the foundations for the utilization of Deep Learning Methodologies that are based on specialized algorithms with the aim of automating the procedures above, thereby facilitating the implementation of these objectives. In this thesis, the role of Color Fundus Photography, SD-OCT, swept source OCT, as well as Widefield or Ultra - Widefield MRI systems for the better evaluation of the periphery of the myopic fundus is analyzed through the prism of Artificial Intelligence Innovations and it provides a contemporary approach in the clinical management of these cases with promising results.

A) INTRODUCTION

The purpose of this study is to assess the impact and effectiveness of deep learning (DL) methodologies that are provided by the advancement of artificial intelligence (AI) tools in the diagnosis, classification and follow-up of highly myopic cases.

Myopic Maculopathy (MM) (often described as myopic macular degeneration-MMD) is a major, non-reversible complication of pathologic myopia (PM) (a severe type of high myopia accompanied by a variety of characteristic maculopathy lesions) that can provoke visual impairment and definite vision loss in affected cases worldwide. High myopia is represented by a significant negative refractive error, i.e. spherical equivalence less than -6.0 diopters, with axial length typically greater than 26.5 mm. While high myopia and pathologic myopia are terms that are frequently used interchangeably, they actually describe different conditions. The appearance of posterior staphyloma along with axial length elongation are the main differentiating elements between high and pathologic myopia. Progression of high myopia and the existence of staphyloma will finally lead to more severe conditions such as atrophic, tractional, or neovascular MM. Myopia can also be related to a series of tissue changes in the eye such as tessellated fundus, atrophy, retinal detachment, lacquer cracks, myopic CNV etc. (Ruiz-Medrano et al., 2019) (Figure 1).

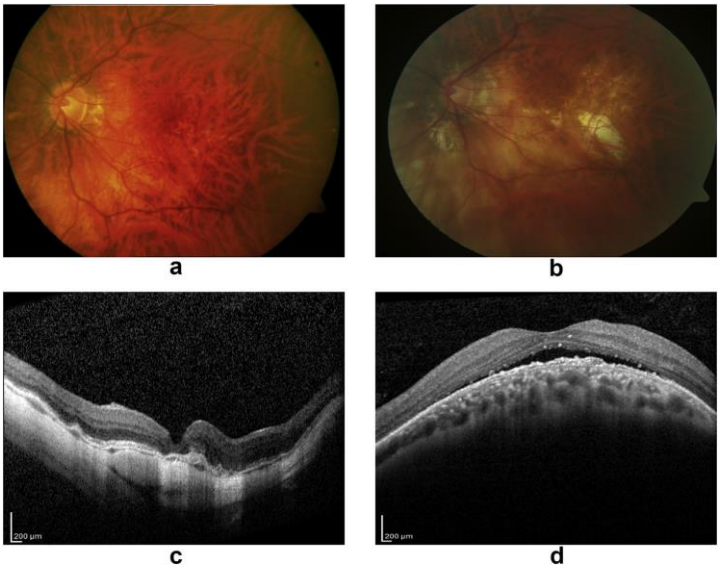

Figure 1: *Fundus photography of a lacquer crack indicated by gradual retinal, choroidal and RPE thinning (a), highlighting the existence of choroidal vessels and sclera (b), OCT scan reveals retino-choroidal thinning and myopic choroidal neovascularization (c), dome-shaped macula formation (d), with hollow sclera and sub macular serous retinal detachment (Ruiz-Medrano et al., 2019).*

According to statistics, approximately 2.45 billion individuals (30% of the global population) are affected by myopia nowadays and it is estimated that by the year 2050 approximately 55.7 million people will present with the side-effect of myopic maculopathy, whereas 18.5 million among them will become blind. These forecasts reveal the epidemic character of the disorder on a worldwide scale, emphasizing the fact that it constitutes a serious public health burden- especially in developed countries of East and Southeast Asia- where the prevalence of myopia among young individuals has reached 80% to 90% in some areas. In approximately three decades (twenty-six years), high myopia is predicted to impact 9.8% of the world's population, a number that sets one billion people at risk for development of sight-threatening complications such as myopic macular degeneration. Therefore, recognizing this risk in advance is of great importance to organize prevention and intervention strategies and avoid vision detriment in these patients. The arguments unfolded above raise the issue of myopia's significant impact on public health and socioeconomic status of each country as well. Indeed, constant acceleration of the urbanization phenomenon, aging and lifestyle modifications render inflammatory and degenerative retinal diseases, such as myopic maculopathy, a threat to global health. Myopic maculopathy- a subcategory of pathologic myopia- is a progressive and irreversible disease, therefore close monitoring and surveillance of the disease's evolution is highly recommended. On the other hand, an insufficient number of myopia specialists worldwide hinders timely diagnosis and restricts close follow-up of highly myopic cases, which is fundamental for early identification of dangerous side-effects. Lastly, various lesions of myopic maculopathy can co-exist in the same eye, leading to interpretation obstacles in image decoding. Thus, recently automated methods with Artificial Intelligence at their core have been proposed to assist physicians and provide a cost-efficient way in managing pathologic myopia patients (Du & Ohno Matsui, 2022).

Many classification systems have been proposed during the last decades; a brief grading from mild to severe (according to the International Photographic Classification and Grading System META-PM) is as follows:

Category 0: No myopic retinal degenerative lesions

Category 1: Tessellated fundus

Category 2: Diffuse chorio-retinal atrophy

Category 3: Extramacular patchy chorio-retinal atrophy

Category 4: macular patchy chorio-retinal atrophy

Also, three kinds of "plus" lesions were described:

Lacquer cracks, myopic choroidal neovascularization (CNV) and Fuchs' spots.

Based on this grading system, eyes of category 2 or greater, or with plus lesions, are defined as having Pathologic Myopia. A more severe type of myopic maculopathy has more marked fundus alterations and worse visual prognosis. Consequently, the timely recognition of these primary modifications in the posterior pole with the assistance of artificial intelligence tools may prove to be mandatory so as to achieve more effective disease stratification and reduction of visual impairment and blindness in these patients (Du et al., 2021).

Several longitudinal studies have been conducted to assess myopic maculopathy progression that is linked to increasing peripapillary atrophy (Figure 2). It must be noted that this condition results from the long-term inflammation of the posterior segment of the eye which leads to gradual visual decrease. Among these, the most thorough was carried out by Hayashi et al., who observed that the early existence of lacquer cracks and staphyloma subsequently influenced the evolution of atrophy, indicating that these features are key points in monitoring the course of the disease. More specifically, the authors described a progression pattern whose first finding is a tessellated fundus which may evolve into diffuse atrophy or lacquer cracks or- less frequently- to myopic choroidal neovascularization (Hayashi et al. 2010). In every situation, the diagnosis typically requires experts' assessment and utilization of different pieces of equipment (multimodal imaging).

The detailed design of automated classification and segmentation models which are based on deep learning algorithms during recent years has optimized the recognition of the characteristic lesions and has increased the accuracy and speed of diagnosis of the disease. This approach might be effective for risk stratification and to identify individuals at higher risk of visual loss. These AI Models use convolutional neural networks (CNNs) and target the facilitation of hospital cases management providing a more complete healthcare service in community. However, unresolved challenges for AI medical studies remain, including lack of transparency, auditability and traceability.

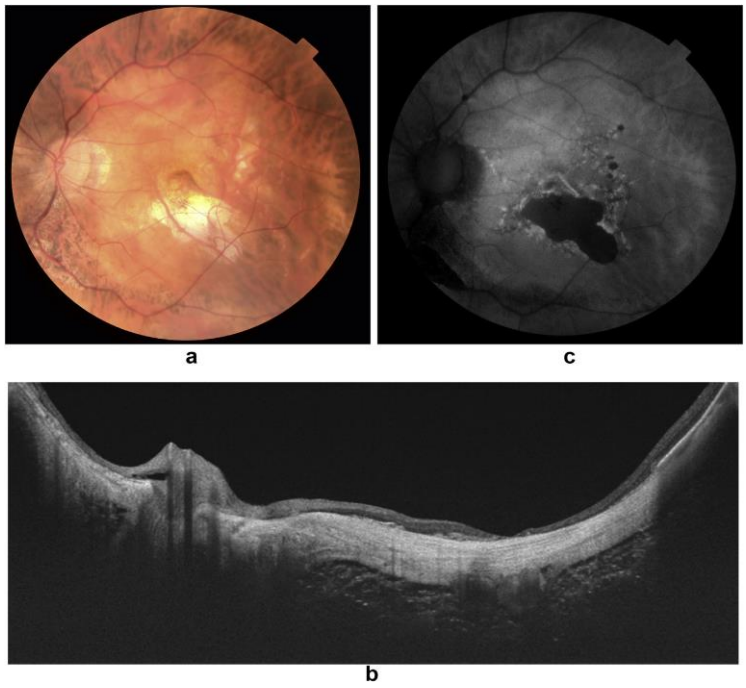

Figure 2: *Color Fundus Photography (a), Swept Source Optical Coherence Tomography (b) and Autofluorescence (c) in a highly myopic patient. Absence of the choriocapillaris is accompanied by reduced autofluorescence and elimination of the RPE and outer nuclear layer (Ruiz-Medrano et al., 2019).*

B) GENERAL CHARACTERISTICS AND GRADING SYSTEM FOR MYOPIC MACULOPATHY

i) Classification Scale for Myopic Macular Degeneration

Even though constituting a major stimulus for visual deterioration worldwide, myopic maculopathy did not include a satisfactory definition for many years. Myopic macular degeneration is a highly complicated disorder, and the different classification systems proposed did not sufficiently cover the numerous modifications that arise in the posterior pole of cases. Therefore, a more complete grading system is required, for a series of reasons. The first one is the exact identification of the stage of the disease that will provide more accurate monitoring and follow-up of the condition's progression. Secondly, consolidation of the currently- available classifications systems would formulate standardized classification criteria that could be applied to compare the results from international multicenter studies. Finally, a more thorough grading system could help to enhance our comprehension of the genetic associations of the disease, which is essential given the widespread use of the terms high and pathologic myopia in genetic research. In order to tackle the issues mentioned above, in 2015 the Meta-

Analysis Study Group for Pathologic Myopia introduced a simplified, uniform grading scale for the disease's more explanatory definition (Ruiz-Medrano et al. 2019).

Historical recap: The first classification system was proposed by Curtin and Karlin, in 1970, who included in the definition of myopic maculopathy the following five features: chorio-retinal atrophy, central pigment spots (Fuchs' spot), lacquer cracks, posterior staphyloma and optic nerve crescent.

The next grading system was introduced by Avila et al. in 1984 in the context of increasing severity from a normal appearing posterior pole (M0) to choroidal pallor and tessellation (M1), with further addition of posterior staphyloma (M2), lacquer cracks (M3), focal areas of deep choroidal atrophy (M4) and large geographic areas of deep chorio-retinal atrophy and bare sclera (M5).

These observations were further developed by Tokoro et al. later, in 1998, who graded myopic maculopathy into four categories: 1) tessellated fundus, 2) diffuse chorio-retinal atrophy, 3) patchy chorio-retinal atrophy and 4) macular hemorrhage, the last one associated or not to myopic choroidal neovascularization.

Later in 2010, Hayashi et al. introduced a new grading system based on the long-term evolution pattern of myopic maculopathy by analyzing 806 highly myopic eyes of 429 patients. In contrast to Tokoro's classification, Hayashi et al. designated lacquer cracks as a separate lesion, not belonging to the category of diffuse atrophy. Also, Tokoro distinguished macular hemorrhages as linked or not to myopic choroidal neovascularization, whereas Hayashi completely integrated hemorrhages into the category of myopic CNV or lacquer cracks. Finally, Hayashi separated patchy atrophy into three subtypes: associated with lacquer cracks, diffuse atrophy and posterior staphyloma.

In 2012, Asakuma annotated myopic maculopathy as the existence of ≥ one of the following: diffuse chorio-retinal atrophy at the posterior pole, patchy chorio-retinal atrophy, lacquer cracks, or macular atrophy.

Given the fact that none of these grading schemes gained global approval due to heterogenous definitions and terminology, an international group of experts in high myopia gathered to develop a simplified, uniform, systematic classification system, based on a meta-analysis of pathologic myopia (META-PM). It was proposed by Ohno-Matsui et al. in 2015 and introduced five separate myopic maculopathy categories (Frisina et al., 2020).

In summary, based on this updated system, lesions of myopic maculopathy are divided into 5 stages (Figure 3): Absence of myopic retinal alterations (category 0), fundus tessellation (category 1), diffuse chorio-retinal atrophy (category 2), patchy chorio-retinal atrophy (category 3), and macular atrophy (category 4).

These groups were determined via long- term clinical observations that followed the evolution pattern and risk for development of choroidal neovascularization at each stage. According to the earlier reports, category 2 was subclassified into peripapillary chorio-retinal atrophy (PDCA) and macular chorio-retinal atrophy (MDCA). Three additional features were characterized as "plus signs": lacquer cracks, myopic choroidal neovascularization and Fuchs' spot. The existence of these "plus signs" has been associated with central vision loss and even though they do not fit into any category, they may emerge from, or coexist in, eyes with any of the myopic maculopathy categories analyzed before.

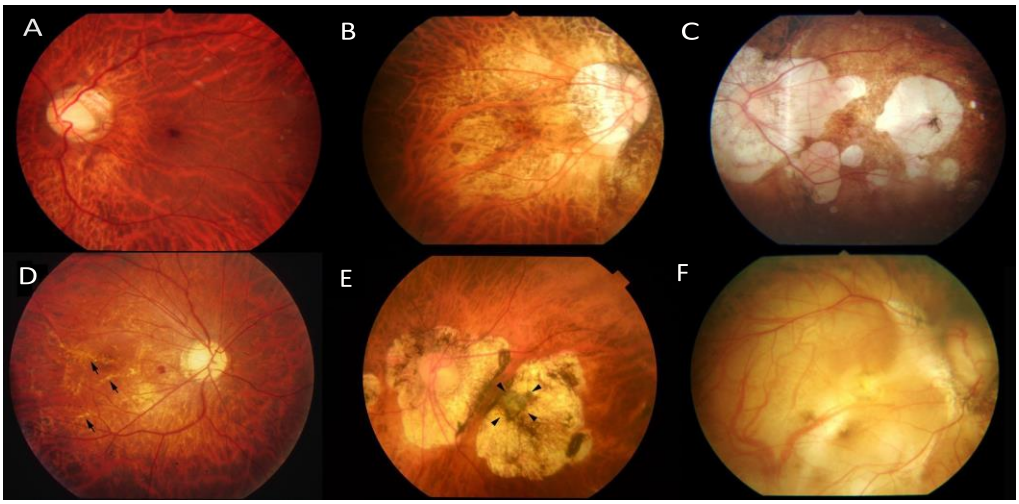

Figure 3: *META-PM Classification of Myopic Maculopathy via Color Fundus Images Analysis. A) Category 1, fundus tessellation. Choroidal vessels are delineated throughout the whole area of the posterior pole. B) Category 2, diffuse atrophy. Yellowish-white and vaguely defined models of atrophy appear in the entire posterior pole. C) Category 3, various lesions of patchy atrophy present as well-defined, grayish-white areas on a background of diffuse atrophy. D) Lacquer cracks (plus sign). Yellowish thick linear patterns, which run in branches or crisscross, are observed in the posterior fundus (arrows). E) Fuchs' spot (plus sign). In the scar phase, myopic CNV is covered by proliferating pigment cells. Afterwards, myopic CNV- related macular atrophy develops resulting from the enlargement of the Bruch membrane rupture around regressed myopic CNV (arrowheads). F) Category 4, a series of lesions of patchy atrophy enlarged and merged contribute in the arising of macular atrophy (Yokoi & Ohno Matsui et al., 2018).*

Based on this new grading system, pathologic myopia is defined as myopic maculopathy of stage 2 or above, the presence of a plus sign, or the existence of posterior staphyloma.

Eyes with macular diffuse chorio-retinal atrophy or with plus lesions were integrated in the severe myopic maculopathy group, while eyes of category 0,1 or those with peripapillary diffuse chorio-retinal atrophy were archived in the less severe type of the disorder. The new ATN classification examines all the aspects of this entity and describes atrophic (A0-no myopic retinal lesions; A1-tessellated fundus only; A2-diffuse chorio-retinal atrophy; A3-patchy chorio-retinal atrophy; A4-complete macular atrophy), tractional (T0-no macular schisis; T1-inner or outer foveoschisis; T2-inner + outer foveoschisis; T3-foveal detachment; T4-full thickness macular hole; T5-macular hole and retinal detachment) and neovascular (N0-no m CNV; N1-macular lacquer crack; N2a-active CNV; N2b- scar or Fuchs' spot) effects to the sclera, choroid and retina of highly myopic eyes.

After several studies, the pathology of myopic traction maculopathy has been interpreted not just as a group of different foveal and retinal changes in a tractional myopic environment, but as a single progressive disorder that encloses diverse stages of evolution (Ruiz-Medrano et al., 2019).

ii) General Features of the Disease

Myopic maculopathy is a highly complex disease that involves atrophic, tractional and neovascular modifications in the posterior fundus of patients. The most essential factors driving myopic maculopathy's progression are axial length elongation, expansion of the posterior eye wall and staphyloma that may lead to irreversible photoreceptor loss and central visual impairment in adults.

The most representative features of the disease are cited below:

1. Retinal, choroidal, and scleral thinning which are usually associated with the presence of posterior staphyloma formation.

2. Tessellated fundus, that results from hypoplasia of the retinal pigment epithelium (RPE) surface and allows clear illustration of the choroidal vascular network in color fundus images. It constitutes a feature that usually appears in younger cases with less myopia, shorter axial length (less than 26 mm) and absence of chorio-retinal atrophy or staphyloma.

3. Diffuse chorio-retinal atrophy, that is usually depicted as a yellowish white area around the optic disc. On fluorescein angiography (FA) it is represented by mild hyper fluorescence in the late phase due to tissue staining. On OCT scans significant thinning of the choroidal layer can be seen, whereas indocyanine green angiography (ICGA) shows significant reduction of the choroidal capillary network. The existence of remaining outer retina and RPE tissue around choroid loss can explain the relatively preserved vision in eyes with diffuse atrophy.

4. Patchy chorio-retinal atrophy that presents as greyish-white lesions in the macula or around the optic disc. The pathogenetic mechanism underlying this stage is a total absence of choriocapillaris and a complete destruction of the outer retina and RPE. In FA and ICGA imaging, a choroidal filling defect is observed around patchy atrophy, that correlates to a loss of the entire thickness of the choroid, RPE and outer retina on OCT scans. Recent swept-source OCT (SS-OCT) or histological studies reveal a discontinuity of Bruch membrane in the regions with patchy atrophy as well as in the peripapillary gamma zone. These defects rename the entity as “macular Bruch membrane rupture”.

Patchy atrophy is subgrouped into 3 classes (Figure 4):

a. Patchy atrophy that emerges from lacquer cracks, P(Lc),

b. Patchy atrophy that grows around an advanced diffuse atrophy, P(D)

c. Patchy atrophy that develops along the edge of a posterior staphyloma, P(St).

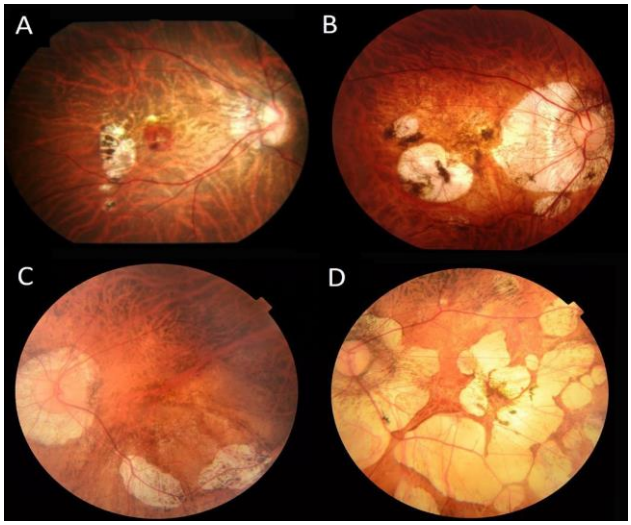

Figure 4: *Three categories of patchy atrophy. A, P(Lc): patchy atrophy that emerges from lacquer cracks and usually has a narrow elliptical form. B, P(D): patchy atrophy that arises within the area of advanced diffuse atrophy, that usually appears as circular or oval. C, P(St): patchy atrophy that can be distinguished along the edge of posterior staphyloma. D, the foveal center might be involved due to enlargement and coalescence of lesions during the final stage of myopic chorio-retinal atrophy. Visual acuity measurement is 0.6 (Yokoi & Ohno Matsui, 2018).*

5. Macular atrophy, that refers to the state of occupation of the entire area of the posterior fundus including the foveal region (macula space) leading to a central vision loss. In this case the posterior pole obtains a “bare sclera” appearance with retrobulbar blood vessels notable through the thin transparent retinal tissue.

6. Choroidal neovascularization is a major complication that occurs in areas of preserved choriocapillaris (higher vascular endothelial growth factor -VEGF- levels in the aqueous humor of these patients) and is more frequent in eyes with less advanced staphylomas. The presence of a Fuchs’ spot (dark area in the macula) is indicative of a late stage myopic CNV (regression of choroidal neovascularization) and is caused by hyperplasia and migration of RPE cells to the subretinal or intraretinal tissue (proliferation of the retinal pigment epithelium that is associated with choroidal hemorrhage). Chorio-retinal atrophy will typically develop around the regressed membrane, leading to a poor visual outcome (loss of two or more lines of the Snellen chart). A timely treatment with anti-VEGF injections is required in these cases to avoid severe visual loss.

7. Myopic macular hole and myopic foveoschisis, induced by tractional changes in the myopic fundus. The development of a full thickness macular hole (FTMH) in severe cases may provoke retinal detachment in these eyes attributed to persistent tractions over its margins (Figure 5).

8. Dome-shaped macula, represented by the ventral configuration of the sclera, and often related to serous, non-evolving retinal detachment (Yokoi & Ohno-Matsui, 2018) (Ruiz-Medrano et al., 2019).

Figure 5: *Myopic traction maculopathy may lead to full-thickness macular hole formation in advanced cases and retinal detachment deriving from constant tractional forces applied over its margins (Ruiz Medrano et al., 2019).*

iii) Evolution of the Disorder, Risk Factors for Progression

Based on Hayashi et al.'s (2010) conclusions, age, increased axial length and staphyloma are the main factors affecting the advancement of diffuse atrophy and thus the aggravation of the myopic macular degeneration status. It was observed that a high percentage of myopic eyes (40%)- especially those with posterior staphyloma- appeared with progressive chorio-retinal atrophy (Figure 6). This finding indicates that posterior staphyloma constitutes a major catalyst in the spreading of atrophy instead of a separate category in the grading system of the disease. As a fact, eyes with posterior staphylomas have a higher tendency of converting progressive tessellation towards diffuse and patchy atrophy. Also, aging plays an important role on an anatomical and functional level in eyes with myopic maculopathy. Several authors have associated more severe types of atrophic myopic maculopathy with a worse

visual acuity and a greater advancement/ merging of atrophic areas, spreading of lacquer cracks as well as development of myopic CNV from a ruptured Bruch's membrane. Moreover, aging is linked to the RPE's health, as a degeneration of the tissue (attenuation with pigment deposits) is noted among elderly people, with removal of atrophic RPE cells in advanced cases. Lastly, anteroposterior elongation can cause gradual thinning and tension on the ocular tissues leading to retinal vessel rectification as well as choroidal and RPE thinning that facilitates visualization of large choroidal vessels. Occlusion of these vessels can provoke fibrosis and photoreceptor loss due to insufficient oxygenation that results in a decrease in retinal thickness and central vision loss.

Briefly, the most usual patterns of the disorder's evolution are from tessellated fundus to diffuse atrophy with lacquer cracks, followed by spreading and coalescence of the atrophic lesions and the gradual conversion of diffuse atrophy into patchy atrophy. Firstly, a spreading of the diffuse atrophic areas occurs which is succeeded by the emergence of atrophic patches. It must be emphasized that patients with patchy atrophy appear with a worse visual prognosis than those with lacquer cracks, particularly when the atrophic areas fuse. To summarize this pathogenetic pathway, diffuse atrophy may progress into atrophic patches or lacquer cracks with or without myopic choroidal neovascularization but also lacquer cracks themselves may lead to focal atrophy or neovascularization. Atrophic lesions can be merged to create geographic areas of atrophy while myopic choroidal neovascularization may convert into regions of diffuse atrophy. These complex pathophysiological mechanisms indicate that there are subtle, interconnected relationships between the various changes/alterations in the fundus of myopic maculopathy cases, a statement that strongly verifies the evolving nature of the disease. The most recent classification system proposed by Ohno-Matsui et al. for myopic atrophy arrived at the following discovery: primary atrophic alterations that include tessellated fundus and diffuse atrophy were typical among younger aged populations that appeared with milder myopia and shorter axial lengths. On the other hand, Hayashi et al. unveiled a correlation between patchy atrophy, longer axial lengths, lacquer cracks and myopic choroidal neovascularization in older patients. This proves that aging is a major factor for aggravation of atrophic areas by inducing enlargement and coalescence of lacquer cracks, which increases the risk of neovascularization. Moreover, perimetric defects

are more common in highly myopic eyes and this is where the contribution of ultra-wide field (UWF) imaging appears useful.

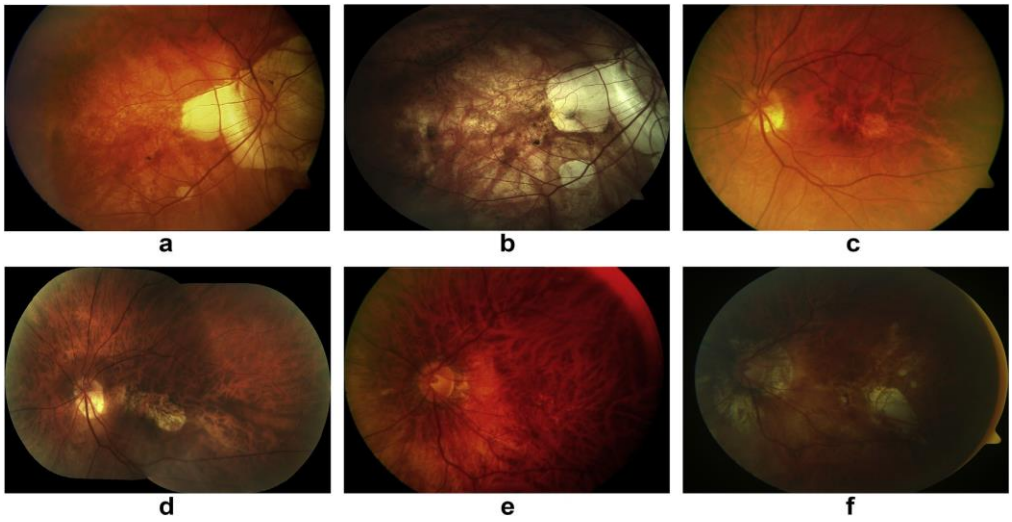

Figure 6: *Chorio-retinal atrophy progression patterns (a, b), edge of the staphyloma (c, d) and lacquer cracks' formation (e, f) based on Tokoro's grading system (Tokoro et al.,1998).*

Hayashi et al. in 2010 proposed a progression scheme that distinguished the defects caused by progressive choroidal thinning -that include progression from a normal to a tessellated fundus and evolution from peripapillary diffuse chorio-retinal atrophy to macular diffuse atrophy- from the changes related to formation and enlargement of Bruch's membrane holes that include: lacquer cracks that convert into patchy atrophy and patchy-related macular atrophy and myopic CNV that progresses into CNV-related macular atrophy.

The progression rate from pathologic myopia to myopic maculopathy is more widespread in eyes with macular atrophy or patchy atrophy due to the existence of holes in Bruch's membrane versus the choroidal thinning that characterizes diffuse atrophy. This acceleration was noticed even in the absence of lacquer cracks or CNV and it was rendered to a deterioration in Bruch's membrane alterations that accompany axial length elongation.

Systemic conditions may also contribute to the advancement of macular atrophy. For instance, increased systemic blood pressure (BP) was recognized by Chen et. al as a risk factor for developing myopic maculopathy since an increase of 10 mmHg in systemic BP raises the probability of disease by a factor of 1.5 in highly myopic cases. This means that patients with more severe types of macular atrophy and mCNV have

typically higher systemic BP compared to patients with less severe macular changes. Moreover, a correlation was found between increased blood pressure and a thinner choroid, which implies that this underlying condition can affect choroidal circulation and aggravate myopic maculopathy's status.

To conclude, a reference will be made to the pathogenetic background of lacquer cracks which are breakings in the RPE -Bruch's membrane- choriocapillaris complex and usually coexist with posterior staphyloma. The additional emergence of mCNV may manifest as a pathologic reply of a remedial mechanism. These lesions appear as multiple yellowish-white irregular lines, usually horizontally- oriented, and can be linear or stellate, occasionally branching or crisscrossing. They are more widespread amongst males and reduce with age. They are depicted as a window defect in Fluorescein angiography where they are represented by hyper-fluorescent tracks without any leakage. On fundus autofluorescence (FAF), a hypo-autofluorescence pattern is observed (Ruiz-Medrano et al., 2019).

Finally, the pathogenesis of myopic traction maculopathy development should not be neglected. It is supposed to be provoked by preretinal factors that manifest as centrifugal and tangential tractions to the retina - i.e., incomplete posterior vitreous detachment (PVD), vitreomacular traction (VMT) and epiretinal membrane (ERM) - and subretinal factors that are associated with centrifugal forces to the retina and lead to deformation of the scleral eyewall. Both can potentially cause destruction to the retina if they exceed its elasticity that is restricted by small retinal vessels, thickened or stiffened internal limiting membrane (ILM) or vitreous remnants.

Additionally, the decreased retinal blood flow that accompanies choroidal and RPE atrophy is supposed to provoke loose adhesions between not only the retinal nerve layers but also the photoreceptors and the RPE itself. An additional factor that accelerates the creation of tractions is partial or complete PVD, that in myopic eyes occurs earlier and more frequently than in emmetropic eyes.

Moreover, in highly myopic eyes, a physiological lacuna can be created in contact with the ILM, between the vitreous cortex and vitreous. This lacuna is named posterior pre cortical vitreous pocket (PPVP) and can provoke a PVD.

According to Lewis et al. (2014) who examined the biomechanics of the sclera in enucleated eyes of young chicks, there are two mechanisms that contribute to scleral deformation in high myopia: elasticity and creep. The pathological elongation of the

eye in myopia is linked to the inhibition of collagen crosslinking, which normally affects the regulation of the eye's refractive development. Reduced scleral rigidity in myopic eyes in comparison to emmetropic ones can be attributable to this phenomenon. This deformation induces an equatorial area extension and a stretching of the globe. The first procedure is related to the emergence of peripheral retinal defects, like white without pressure, pigmentary, paving stone and lattice degeneration. The second one is related to an ectasia of the sclera, that causes the development of posterior staphyloma which can involve the optic nerve and/or the macular area, but can also appear laterally (Frisina et al., 2020).

iv) Imaging Techniques for Diagnosis and Monitoring of Disease

The precise diagnosis and evaluation of pathologic myopia requires thorough investigation and is aided by a series of imaging techniques, including fundus photography and OCT. Indeed, the adoption of the OCT imaging modality gave access to the posterior vitreoretinal anatomy, which allowed the recognition of subtle macular modifications, such as retinoschisis, lamellar holes and shallow macular detachment. In this way, the crucial role of the retinal traction generated by ERM formation, as well as the role of VMT, were highlighted in the emergence of myopic maculopathy.

It is a fact that OCT is a widely used, noninvasive method for detecting retinal disorders, constituting the general examination method to assess the retina of myopic patients. The contribution of this technique facilitated the precise definition of the ultrastructural features and the tractional modifications that take place in myopic maculopathy, but also permitted to monitor the progressive nature of the disease in the long run.

In 2004 Panozzo introduced the concept of myopic traction maculopathy (MTM) to describe the total of foveal tractional changes in highly myopic eyes. MTM included the following disorders: foveoschisis/ maculoschisis/ retinoschisis (FS/MS/RS), retinal/ foveal detachment (RD/FD), lamellar macular holes (LMH) and full-thickness macular holes (FTMH) with macular hole retinal detachment (MHRD) or without RD. Based on his classification system, this entity is generated by epiretinal tractional forces, is magnified by the appearance of posterior staphyloma and can co-exist with other

degenerative non-MTM pathologic alterations such as choroid atrophy, retinal thinning, lacquer cracks, choroidal neovascular membranes, spontaneous foveal hemorrhage and macular holes, accompanied or not by posterior retinal detachment.

Moreover, according to an analysis of OCT images based on 125 eyes with high myopia that focused on epiretinal tractions (ERM, VMT) and retinal damage (retinal thickening, MS/RS, RD, LMH), a significant prevalence of epiretinal forces (46.4%) and retinal damage (34.4%) was observed on these eyes (Figure 7).

Myopic traction maculopathy is usually asymptomatic in early stages and difficult to identify biomicroscopically. OCT allows to detect minimal macular changes in a primary stage and therefore constitutes an essential tool in the follow-up of the disease. The recommended MSS staging system based on OCT findings, has allowed a more profound comprehension of myopic traction's maculopathy pathogenesis and has provided precise indications on prognosis and management (Frisina et al., 2020).

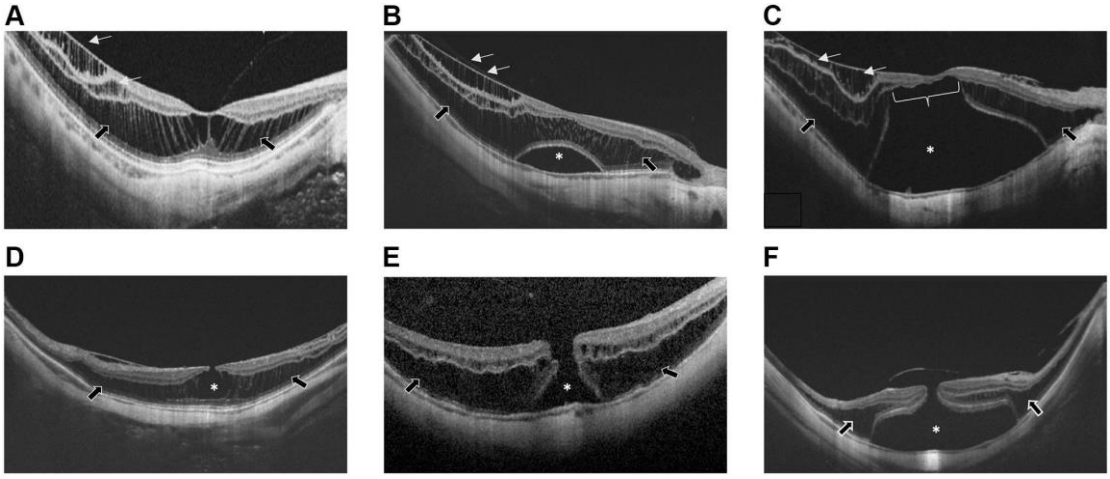

Figure 7: *A) Foveoschsis/ maculoschisis/ retinoschisis (FS/MS/RS). A separation of retinal layers, that remain united by Muller cells stretched in multiple columnar structures is apparent in both inner (white arrows, inner RS) and outer retinal layers (black arrows, outer RS) B) Foveal detachment (FD), indicated by the asterisk. White arrows mark the inner RS, whereas black arrows mark the outer RS C) Retinal detachment (RD) (asterisk) associated with inner (white arrows) and outer RS (black arrows). White line signals an outer lamellar macular hole (O-LMH) D) Lamellar macular hole (LMH). Asterisk indicates the partial foveal defect with intact outer retinal layers. Black arrows demonstrate the outer RS E) Full- thickness macular hole (FTMH). Asterisk indicates the FTMH linked with outer RS (black arrows). F) Full-thickness macular hole accompanied by retinal detachment (MHRD). Asterisk shows the MHRD associated with outer RS (black arrows) (Frisina et al., 2020).*

According to Yu's observations, who assessed the posterior pole curvature of eyes with myopic traction maculopathy in OCT imaging, sharp-pointed shape modifications in the foveal area can promote the disease's progression in highly myopic eyes. This

finding is consistent with the assumption that scleral stretching due to globe expansion and the presence of staphyloma constitute key factors in the emergence of macular epiretinal tractions and the aggravation of vitreomacular adhesions. However, the OCT scan access was confined to the macular area, and the precise configuration of the entire posterior segment of the eye was not acquired. Moreover, the deep excavation of the posterior part of highly myopic eyes prevents us from obtaining distinct OCT images. This is where the utilization of three-dimensional magnetic resonance imaging (3D MRI) appears useful as it has been proven to be appropriate for the examination of eye shape over a wide area that can encompass even a large posterior staphyloma. This technique allows experts to view a staphyloma from any angle and approach the eye globe via various perspectives to extract a valid diagnosis (Yu et al., 2018).

These more advanced techniques (3D-MRI, OCT and UWF imaging) are useful diagnostic instruments, compared to Ultrasonography (US), in the evaluation of a large staphyloma, allowing to visualize and reconstruct the shape of the entire ocular globe, considering the hypothesis that this entity is linked to the appearance of MM, through the inducement of mechanical damage to the retina and optic nerve (Yu et al., 2018).

The discoveries described above are further supported by a clinical study (morphological and quantitative assessment of myopic maculopathy with the assistance of 3D MRI) that was published in 2018 under the auspices of Zhongshan Ophthalmic Center (Hospital of Sun Yat-sen University) in China. The research was conducted by Yu X. et al. and arrived at the conclusion that non-symmetrical globe elongation and staphyloma development can play a crucial role in the generation of myopic traction maculopathy. The methodology applied to derive this result was the following: 103 eyes in total from 65 patients that presented with high myopic maculopathy were examined with the use of 3D-MRI and SD-OCT. Afterwards, the participants were separated into two groups, MTM and non-MTM eyes based on SD-OCT imaging findings. Next, volume renderings and morphology analysis of the 3D MRI of the eyeball were acquired and a quantitative analysis was performed via calculation of vitreous volume and the three-dimensional diameters of the eye globe in three cardinal axes. More specifically, the following four parameters were assessed: vitreous volume, equatorial diameter (ED), anteroposterior diameter (axial length, AL) and the ratio of anteroposterior/equatorial diameter (AL/ED) (Figure 8).

Subsequently, the eye shape distribution and the diameters of the eyeball were compared between the two categories mentioned above. Eye shape distribution, vitreous volume and eye-ball diameter were evaluated between MTM and non MTM eyes. As a result, a significant difference was observed in the eye shape distribution (P<0.01) between the two categories since most of the MTM eyes had undergone a non-uniform expansion (less symmetrical globe shape) of the eyeball, whereas the non-MTM eyes had expanded symmetrically. Nevertheless, no significant difference (P>0.05) was observed neither in the vitreous volume nor in the other diameters between the two groups, although the refractive error (spherical equivalent) of the non-MTM group was more myopic than that of the MTM group (P<0.05) (Yu et al., 2018).

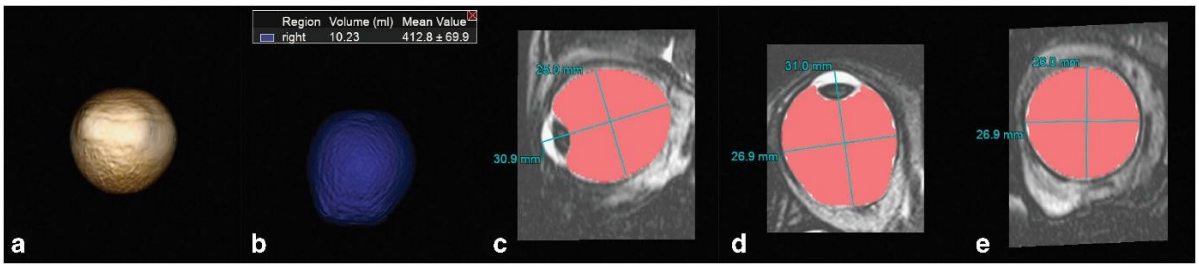

Figure 8: *3D MRI volume versions of the eye and quantitative analysis of the vitreous volume, anteroposterior diameter, axial length (AL) and equatorial diameter (ED) (Yu et al., 2018).*

Another study worth mentioning was published in Acta Ophthalmologic in 2022 and addressed the issue of UWF Imaging in the evaluation of long-term alterations in highly myopic fundus. The purpose of this research was to assess the effect of posterior staphyloma located with the assistance of ultra-widefield fundus imaging on the advancement of myopic maculopathy in highly myopic cases in the long run. The methodology followed in this observational cohort study included monitoring of highly myopic patients for at least five years who were analyzed for fundus abnormalities and the progression of myopic maculopathy according to the international META-PM grading system. It is a fact that compared to conventional fundus photography, ultra-widefield fundus imaging provides a much wider field of view, covering up to 200 degrees of the fundus. This capability offers a strong benefit in the evaluation of myopic maculopathy aggravation and posterior staphyloma recognition. Moreover,

UWF fundus imaging appears essential in documenting peripheral retinal lesions, which are frequently pointed out in eyes with increased axial length (Oh et al., 2022). This study reviewed medical records of highly myopic patients who underwent UWF fundus imaging at the Retina Center of Seoul National University Hospital between July 2012 and December 2014. A complete ophthalmic evaluation was performed, including best corrected visual acuity (BCVA), slit lamp examination, fundus examination, refractive error, axial length measurement, and UWF fundus imaging. Posterior staphyloma was identified based on the presence of abnormal pigmentary changes in the pseudo-color image or the finding of abnormal reflectance, in the red or green separation image, along the staphyloma border (Figure 9) (Oh et al., 2022).

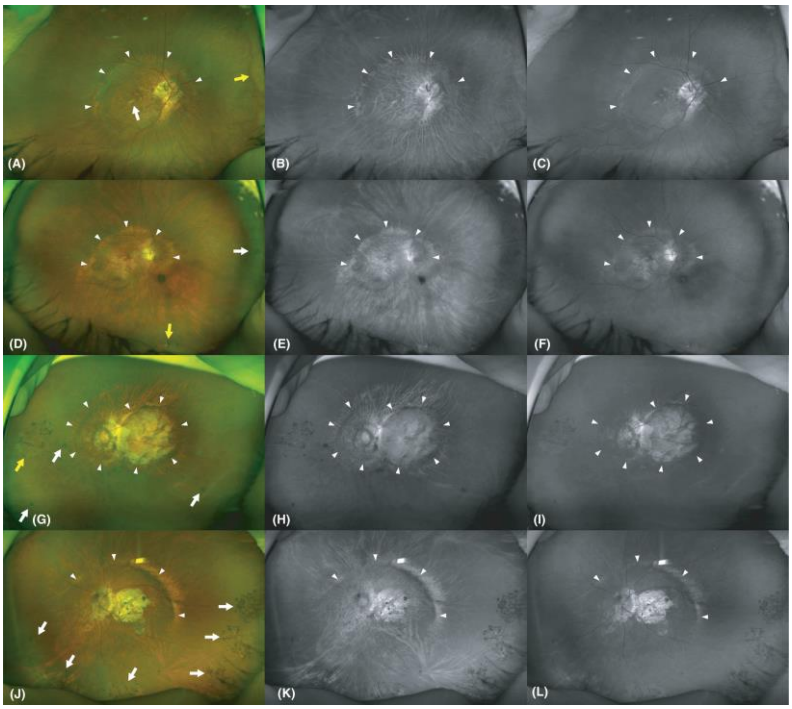

Figure 9: *Myopic maculopathy, posterior staphyloma and peripheral retinal lesions in the pseudo-color (A, D, G, J), red separation (B, E, H, K) and green separation (C, F, I, L) images using ultra-widefield fundus modality. The borders of the posterior staphyloma are annotated by arrows in every image. (A-C) A case of a 57-year-old man of category 1 myopic maculopathy (fundus tessellation) with lacquer crack (white arrow in A). White without pressure is marked in the nasal periphery (yellow arrow in A). (D-F) A case of a 70-year-old woman of category 2 myopic maculopathy (diffuse chorio- retinal atrophy). Pigmentary degeneration (white arrow in D) in the nasal periphery and paving stone defects in the inferior periphery (yellow arrow in D) are detected. (G-I) A case of a 59-year-old woman with myopic maculopathy of category 3 (patchy chorio- retinal atrophy). Note the two adjacent staphylomas, one principally involving the macula and the other involving the optic disc. Areas of diffuse atrophy are restricted within the macular staphyloma, and patchy atrophic lesion is noted along the edge of inferior staphyloma. Pigmentary (white arrows in G) and paving stone degenerations (yellow arrow in G) are apparent in the nasal periphery. (J-L) A case of a 74-year-old woman with category 4 myopic maculopathy (macular atrophy). Multiple paving stone degenerations are emphasized in the nasal and inferior periphery (arrows in J) (Oh et al., 2022).*

The categorization of posterior staphyloma was divided into five forms: wide macular, narrow macular, nasal, peripapillary, and inferior with reference to the grading system proposed by Ohno-Matsui in 2014. With a start point of a 50° conventional fundus photograph captured in the same patient, a corresponding circle of 50° view centered on the macula was overlapped on the ultra-widefield fundus image to evaluate its relative location to the border of posterior staphyloma or the diffuse and/or patchy chorio-retinal atrophic lesions (Figure 10). In this way, the simultaneous identification of peripheral retinal lesions, such as white-without pressure, lattice degeneration, pigmentary or paving stone degeneration and retinal tear or hole, was also executed using ultra-widefield fundus images assessment (Oh et al., 2022).

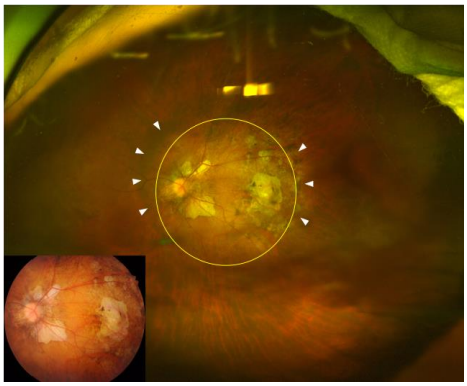

Figure 10: *Ultra-widefield fundus image of a 66-year-old woman with category 3 myopic maculopathy, overlapped with a macula-centered 50° view circle corresponding to the conventional fundus photograph (inlet). The border of posterior staphyloma-wide macular type- is marked by white arrows, whereas patchy chorio-retinal atrophic lesions are detected out of the 50° view circle (Oh et al., 2022).*

The main criteria used for determination of myopic maculopathy's progression were based on a comparison between the initial and final ultra-widefield images and comprised of the following observations during the monitoring period of the cases involved:

1. advancement to a higher grading level
2. for categories 2-4, spreading or proliferation in the amount of maculopathy lesions
3. New emergence or extension of the plus lesions. Moreover, a similar progression was recorded in peripheral retinal alterations during the follow-up period, as signified by an augmentation in the number or size of pre-existing lesions amongst cases (Oh et al., 2022).

Ultra-widefield Fundus Images were evaluated by two retinal specialists for myopic maculopathy, posterior staphyloma, relative location of the border of the staphyloma or chorio- retinal atrophy with the 50° view circle, and peripheral retinal lesions. To avoid deviations, the final decision was extracted after negotiations with senior investigators. As a result, agreement between different diagnostic results was ≥ 90% and kappa coefficient was noted ≥ 0.80% for all parameters. The methodology used for comparison between the myopic maculopathy categories (clinical and ocular characteristics) was one-way analysis of variance or chi-square test (Oh et al., 2022).

During the follow-up period, myopic maculopathy progression was observed in 202 of 390 eyes (51.8%) in total. This advancement appeared in 68 out of 126 eyes (54.0%) with myopic maculopathy of category 2, in 82 of 86 eyes (95%) with category 3 myopic maculopathy and in all 31 eyes (100%) with myopic maculopathy of category 4. Amongst eyes with category 1 myopic maculopathy, all eight eyes with plus lesions and 13 of 122 eyes (10.7%) without plus lesions exhibited progression. None of the eyes with category 0 at baseline demonstrated advancement. Eyes that presented with evolution of the disease during monitoring fulfilled the following conditions: older age (55.7 ± 14.1 versus 47.4 ± 18.7 years; p<0.001), worse BCVA (0.83 ± 0.70 versus 0.32 ± 0.32; p<0.001), and longer axial length (31.1 ± 2.0 versus 29.2 ± 2.1 mm; p<0.001), but similar follow-up period (69.4 ± 7.6 versus 68.8 ± 7.4 months; p=0.433) compared to those that remained stable. Aggravation of myopic maculopathy was significantly more widespread in the eyes accompanied by posterior staphyloma as opposed to those without (142/198 [71.7%] versus 60/192 [31.3%]; p<0.001), whereas the eyes with wide macular type staphyloma showed the most frequent progression between them. Representative images capturing this phenomenon are depicted in Figure 11 (Oh et al., 2022).

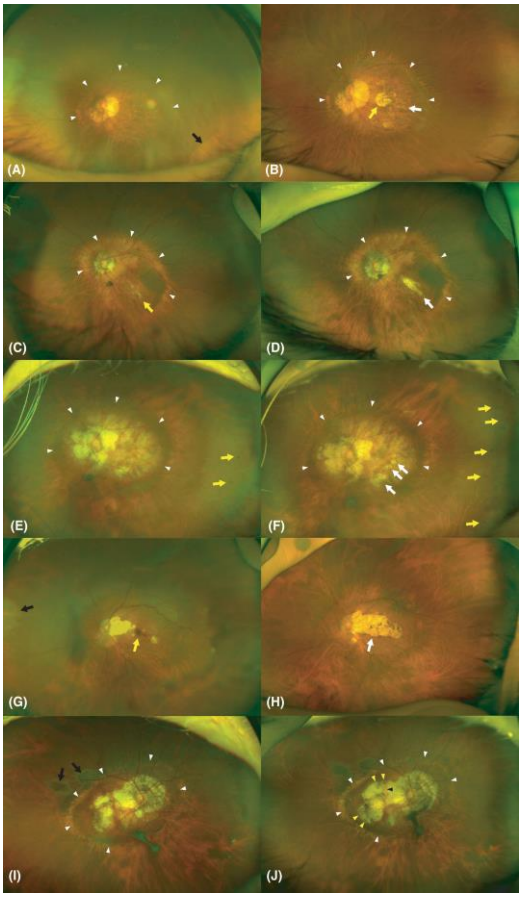

Figure 11: *Characteristic ultra-widefield fundus images visualizing the advancement of myopic maculopathy. Note the pigmentary defects at the border of the posterior staphyloma in every image (white arrows). (A, B) A 57-year-old man with tessellated fundus, appeared with a stellate lacquer crack (white arrow in B) and patchy atrophy (yellow arrow in B) 76 months later. White without pressure is noted in the inferonasal periphery (black arrow in A). (C, D) A 72-year-old woman with diffuse chorio-retinal atrophy and lacquer crack (yellow arrow in C) presented with patchy atrophy (white arrow in D) 66 months later. (E, F) A 69-year-old woman with patchy atrophy demonstrated enlargement and new emergence of lesions (white arrows in F) 80 months later. Pigmentary alterations in the temporal periphery were noted (yellow arrows in E and F). (G, H) A 65-year-old woman without posterior staphyloma appeared with patchy atrophy and myopic choroidal neovascularization (yellow arrow in G). After 78-month follow-up, choroidal neovascularization-related macular atrophy (white arrow in H) emerged. White-without pressure is marked in the nasal periphery (black arrow in G). (I, J) A 70-year-old woman with macular atrophy showed enlargement of atrophic areas (yellow arrowheads in J) 76 months later. Pigment degenerations were noted in the mid-periphery of the fundus (black arrows in I). Attenuation of a large blood vessel was apparent in the area of chorio-retinal atrophy during monitoring (black arrow in J) (Oh et al., 2022).*

The frequency of progression or development of new peripheral lesions during follow-up did not differ between the different categories of myopic maculopathy (p=0.25).

Discussion: In this hospital-based study, 390 highly myopic eyes were followed-up using ultra-widefield fundus imaging for longer than 5 years. This imaging modality offers a wider field of view compared to conventional fundus photography and

facilitates the more precise documentation of the extent of chorio-retinal atrophic lesions and the presence of posterior staphyloma or peripheral retinal lesions. During a mean monitoring period of 69.2 months, advancement of myopic maculopathy was observed in 51.8% of eyes and was significantly associated with the presence of posterior staphyloma. The conclusion of this study indicates that recognizing the existence of posterior staphyloma and the full extent of chorio-retinal atrophy based on ultra-widefield fundus imaging may play a significant role in the clinical follow-up of highly myopic cases by detecting the pathologic alterations in the posterior pole.
Although there is no tangible proof, it is assumed that stretching of the choroid tissue due to expansion of the sclera within the staphyloma is a possible underlying pathophysiological mechanism for myopic maculopathy progression compared to highly myopic eyes without staphyloma. Moreover, it has been noted that longer axial length constitutes a strong risk factor for the aggravation of the disease (advancement of the lesions) which indicates that structural changes in the eyeball shape can independently affect the progression of the characteristic alterations in myopic macular degeneration (Oh et al., 2022).

To conclude, the type of posterior staphyloma (specifically the wide macular type, whose border is least likely to be included within the view of conventional fundus imaging), can be determined more easily via ultra-widefield photography and is linked with a higher progression rate of myopic maculopathy and emergence of new atrophy patterns in the posterior pole.

Additionally, despite the relatively short follow-up period of the study, a similar progression rate in the category ≥ 2 myopic maculopathy with two recent observational studies based on the META-PM classification suggests that monitoring based on ultra-widefield fundus imaging may be more sensitive for the detection of expansion or modification in chorio-retinal atrophic lesions, probably because large chorio-retinal atrophic lesions do not fit within the 50° view of conventional fundus photography. Another possible explanation may be that progression of myopic maculopathy might be accelerated in the eyes with pathologic myopia, which corresponds to category ≥2 or the presence of plus lesions (Ohno Matsui et al., 2015) and can be detected with an interval of only a few years (Oh et al., 2022).

In every situation, the results of the studies analyzed above enlighten in a unique way the utility of the 3D-MRI and ultra-wide-field fundus modalities in the monitoring of the evolution of myopic maculopathy in highly myopic cases, highlighting them as essential tools in the first screening of these patients.

Lastly, according to an article published on 8 June 2022 by Yong Li et al. relating the advances in OCT imaging in Myopia and Pathologic Myopia, especially the development of swept-source OCT, widefield or ultra-widefield systems, have greatly contributed to the comprehension, diagnosis and treatment of myopia related complications. The OCT imaging technique has enhanced the illustration of vitreous properties and measurement of choroidal thickness in myopic eyes. Widefield OCT systems have greatly improved the visualization of peripheral retinal lesions and have enabled the detection of wide staphyloma and estimation of ocular curvature, since ultra-widefield swept source optical coherence tomography (SS- OCT) can scan a field of view up to 100° of the retinas. More explanatory, ultra-widefield OCT can visualize the staphylomatous contour of highly myopic eyes, generating detailed imaging of the vitreomacular interface and progressive lesions of myopic traction maculopathy.

Moreover, the use of SD-OCT revealed an association between the degree of myopia and the change of retinal thickness. An increase in myopia was correlated with foveal thickness growth and decrease in inner/outer macular thickness. SS-OCT imaging unveils defects in the morphology of Bruch's membrane, represented by a lack of Bruch's membrane, choriocapillaris, photoreceptors and RPE. In the case of atrophic myopic maculopathy, choroidal thinning due to patchy atrophy formation is represented in optical coherence tomography angiography (OCTA) imaging by a loss of the choriocapillaris flow signals (Figure 12). (Li et al., 2022).

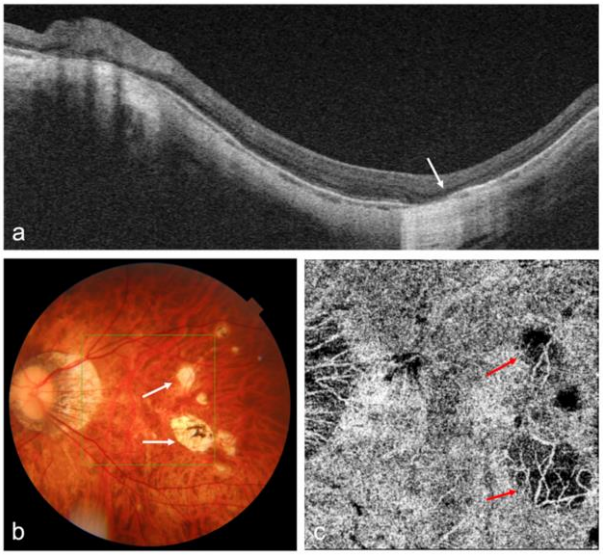

Figure 12: *OCT/OCTA images and fundus photography of a myopic maculopathy case with patchy chorio-retinal atrophy. A) Swept-source OCT image depicts the absence of RPE, choroid and Bruch's membrane around patchy atrophy. B) Color fundus photograph demonstrates areas of patchy chorio-retinal atrophy (white arrows) C) OCTA image depicts the loss of choriocapillaris flow signals corresponding to areas of patchy atrophy formation (red arrows) (Li et al., 2022).*

C) CONTRIBUTION OF ARTIFICIAL INTELLIGENCE TOOLS

i) General Remarks

Myopic Maculopathy deriving from pathologic myopia evolution is a major cause of severe vision detriment and blindness worldwide and can irreversibly affect a patient's visual acuity. Inability to diagnose and treat the disease in a timely manner can often result in reduced quality of life and increased financial burden for these cases. The availability of ophthalmologists specializing in fundus diseases is often inadequate, especially in developing countries and some underdeveloped areas, which can impede treatment options in remote areas. In recent years, artificial intelligence systems have been gradually applied to screen, diagnose, classify, and guide the treatment of retinal diseases, which can greatly reduce the human and material resources required for conventional screening modalities. They can also be used to recognize optical bioimaging markers in myopic maculopathy cases, favoring early diagnosis and treatment.

Artificial Intelligence Techniques typically utilize Fundus Photographs or Optical Coherence Tomography Images, which are the most frequently preferred imaging methods since they are non-invasive and can be easily performed in everyday clinical practice, to extract meaningful data with the assistance of convolutional neural networks concerning lesions recognition and prediction values assessment. Their introduction in managing high myopic patients holds high clinical value since hospital data acquisition from human experts hides imperfections and uncertainties. Moreover, scientific research in this field requires a strong validation/ verification process as well as reliable testing with evidence-based hypotheses that can be provided via artificial intelligence tools' contribution.

Machine learning (ML) techniques offer a supplementary advantage since they can reshape results even closer to the true value. Physicians conducting research must manage a large volume of data and filtering out representative features or measurements is not always an easy task. Machine learning algorithms provide an innovative alternative to traditional methods such as principal component analysis (PCA) to achieve data dimension reduction. Some of them include spectral embedding, iso map embedding, randomized singular value decomposition-based PCA and others. These approaches supply physicians with reference data to help them tackle complex situations, but also facilitate screening of high myopia cases in rural suburbs where myopia experts or essential equipment are out of reach.

Deep Learning (DL) Techniques are a sub-type of Artificial Intelligence that include multiple levels of representational learning (additional hidden layers) that fundamentally assist in the management of more complicated nonlinear patterns and can therefore ameliorate data handling on a large scope. These techniques have sparked tremendous global interest during recent years, making AI a key component of the fourth Industrial Revolution in mankind's history. A primary benefit of their introduction could be in screening, diagnosis but also monitoring of high-risk patients for the advancement of myopic macular degeneration (i.e. in eyes with existing myopia). Moreover, their perspective unlocks the door of machine learning from raw datasets, giving access to automatic discovery of complex features that are crucial in

the classification process of the disease. In other words, this type of algorithms' deployment allows the analysis and process of input data without mediation of manual feature engineering and permits in this manner automatic recognition of representative structures included in the disease's spectrum via a multimodal imaging process. One of the most effective DL architectures is the convolutional neural network (CNN), which has been specifically designed for analyzing medical images. CNNs are an advanced type of Artificial Neural Network (ANN) which is inspired by the biological brain's architecture, consisting of one input layer, responsible for passing the data to the network, and multiple hidden layers (the final being the output information layer). Several CNN models, such as Alex Net, VGG Net, Res Net, Inception, Dense Net, and Efficient Net have been developed to enhance the accuracy measurements in controversial medical images. Deep learning algorithms have demonstrated enormous potential in automated analysis of medical information and imaging properties, across a variety of medical disciplines. A key challenge for deep learning studies is the management of diverse datasets from different countries and centers for algorithm development. Data transfer between collaborators is often limited by restrictions due to privacy and data security. Additionally, transparency regarding model validation and testing results for many published deep learning systems proves to be insufficient. Blockchain technology could be a potential solution to this problem via adopting the role of a shared ledger for data management in a decentralized, secure and trusted manner, and providing traceability and auditability for reporting testing results. Successful integration of deep learning and blockchain technology might help to enhance efficiency, automation, and data security and privacy, and ameliorate the quality of AI medical research (Du et al., 2021).

As mentioned before, one of the main sections of Artificial Intelligence is Machine Learning, which can effectively be used to perform statistical analysis, manage large amounts of data, and discover relationships between different biological characteristics. A distinguishing functional characteristic of this sub-field is its flexibility of encompassing algorithms capable of learning from raw data, without being explicitly programmed. Machine Learning Techniques can detect different categories of myopic maculopathy and consist of supervised learning, semi-supervised and unsupervised learning. Some of the indicative methods applied are kernel ridge regression, support

vector machines (SVM), nearest neighbors, gaussian processes, naïve Bayes, random forests, neural networks and others. Evolutionary methods such as extreme gradient boosting (XG Boost) and light gradient boosting machine (Light GBM) are used to improve regression models and can activate prediction patterns regarding advancement of high and pathologic myopia (Du & Ohno Matsui, 2022).

Artificial intelligence models for multi-disease classification based on conventional retinal fundus images have matured on a large scale during the last years. However, color fundus photography has a small imaging range and requires a time-consuming pupil dilation preparation. Ultra-wide field fundus images have a wide imaging range, acquiring 200° fundus images in a single scan, and have the benefit of being noncontact, pupil-dilation-free, and easy to use. This technique offers the advantage of much more rapid screening of fundus diseases.

Several studies have been designed, that train a series of deep learning algorithms and AI- models based on the META-PM classification system using a large dataset of color retinal fundus images and OCT imaging obtained from the ophthalmic clinics of hospitals and annotated by expert teams. These models could: 1) recognize pathologic myopia cases, 2) define the category of myopic maculopathy 3) discriminate and localize the “Plus” lesions automatically and 4) carry out successful risk stratification to identify the severe cases that need more immediate intervention.

ii) Methodology of the Review

In this review, 2.888 studies in total were identified by navigating into three different databases (PubMed, ScienceDirect- Elsevier and Google Scholar), out of which only 774 records were finally screened after removing duplicate entries and ineligible registrations via automation tools.

The search on the platforms was executed with the aid of a specific algorithm, i.e. (“Artificial Intelligence” OR “AI” OR “Machine Learning” OR “ML” OR “Deep Learning” OR “DL” OR “Artificial Neural Networks” OR “ANN” OR “Convolutional Neural Networks” OR “CNN” OR “Automated Diagnosis” OR “Automated Screening” OR “Automated Classification” OR “Follow-Up” OR “Disease Progression”) AND (“Myopic

Maculopathy" OR "Myopic Macular Degeneration" OR "MM" OR "High Myopia" OR "Pathologic Myopia") which was adapted to the search needs of each different platform used.

The selection of the studies was carried out with the assistance of specific inclusion and exclusion criteria (Table 1) that were determined prior to the launch of the online search, after deducting 756 studies on a first level by reading titles and abstracts.

Table 1: *Overview of the inclusion and exclusion criteria for screening and selection.*

Inclusion Criteria	1.Studies investigating myopic maculopathy or its subtypes 2.Studies using at least one of the following techniques: Artificial Intelligence (AI), Machine Learning (ML), or Deep Learning (DL) 3.Studies providing information on evaluation metrics such as sensitivity (SEN), specificity (SPE), accuracy, area under the curve (AUC) 4.Studies published between the years 2018 and 2024.
Exclusion Criteria	1.Studies that do not use any AI, ML, or DL techniques 2. Non-human subject research 3.Conference abstracts or presentations 4. Reviews, meta-analyses, letters, editorials, surveys and case reports 5. Articles without full text available 6. Studies not published in English 7. Studies published outside the years 2018 to 2024.

Following the initial selection process, 18 studies were thoroughly reviewed in full text for eligibility. Of these, 13 were selected for inclusion and further analysis in the thesis based on their relevance and contribution to the research topic.
The successive stages of the methodology followed are demonstrated on the PRISMA flow diagram (Page et al., 2021) that is illustrated below (Figure 13).

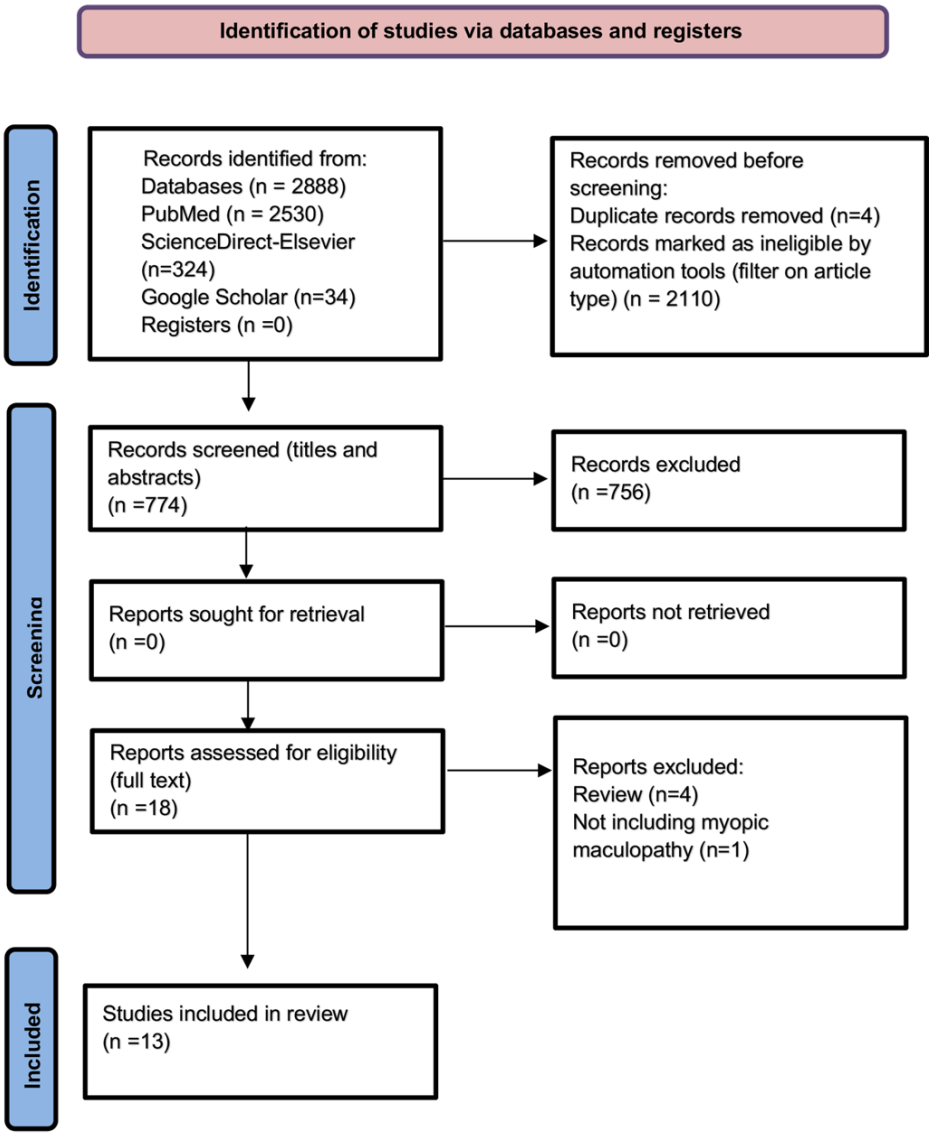

Figure 13: *PRISMA flow diagram.*

Data extraction of results: An independent data extraction procedure was performed by the author among the selected studies using a predefined customized form that captured the following details: Author, Year, Country, Diseases Included, Problem Type, Number of Images/eyes, Imaging Modality, AI Algorithms and AI Models Performance (Table 2). To create this data extraction table, studies were evaluated in their full text and afterwards conclusions were drawn according to the literature research conducted. These papers provided a valuable source of information and allowed stemming of key messages via a critical analysis process regarding the theme

under discussion. Table 2 constitutes a characteristic representation of the procedure described above.

***Table 2**: Summary of Analyzed Studies and Their Reported Performance Metrics.*

Author	Country	Diseases Included	Problem Type	No of images/ eyes	Imaging Modality	AI Algorithms	AI Models Performance
Tan et al. (2021)	Singapore, China, Taiwan, India, Russia, UK	Myopic Macular Degeneration, High Myopia	Detection, Risk Stratification, Screening	226.686 images	Retinal Photography	ResNet-101	**For MMD (internal test):** AUC:0.978, Sensitivity:91.4%, Specificity:94.2% **For MMD (external test):** AUC:0.969-0.988, Sensitivity:96.8%-98.4%, Specificity:85.5%-95.9% **For High Myopia (internal test):** AUC:0.978, Sensitivity:91.3%, Specificity:94.5% **For High Myopia (external test):** AUC:0.913-0.966, Sensitivity:85.3%-97.8%, Specificity:76.4%-95.5%
Du et al. (2021)	China	Pathologic Myopia, Myopic Maculopathy	Feature Mining, Severe Myopic Maculopathy Classification	457 eyes	CFP	ML with radiomics, Random Forest	AUC:0.8263 for new radiomics features, AUC:0.7925 for clinic features, AUC:0.8358 for combined features
Lu et al. (2021)	China	Pathologic Myopia, Myopic Maculopathy	Grading, Diagnosis, Detection, Classification	32.010 images	CFP	ResNet-18, Faster R-CNN+FPN	**Algorithm I:** AUC:0.995, Accuracy:0.973, Sensitivity:0.939, Specificity:0.981 **Algorithm II:** Macro-AUC:0.979, Accuracy:0.967, Kappa:0.988 **Algorithm III (for "Plus" lesions):** Accuracy:0.970-0.994, F1 Score:0.685-0.889
Ye et al. (2021)	China	Myopic Maculopathy	Diagnosis, Detection, Classification	2.342 images	OCT	ResNeSt101	AUC:92.7%-97.4%, Sensitivity:73.9%-92.8%, Specificity:84.8%-94.0%
Du et al. (2022)	Japan	Myopic Traction Maculopathy, Dome-Shaped Macula, Myopic Neovascularization	Diagnosis, Grading	9.176 images	SS-OCT	Darknet-19	**MTM Model**: AUC:0.946, AUPR:0.876 **DSM Model**: AUC:0.978, AUPR:0.653 **MNV Model**: AUC:0.985, AUPR:0.908
He et al. (2022)	China	Myopic Maculopathy	Classification	3.400 images	OCT	Transfer learning, ResNet-18	**Test Dataset:** AUC:0.986, Accuracy:96.04%, Kappa:0.940 **External Validation Dataset:** AUC:0.938, Accuracy:90.6%, Kappa:0.897
Tang et al. (2022)	China	Pathologic Myopia, Myopic Maculopathy	Diagnosis, Grading, Segmentation, Monitoring of progression	1.395 images	CFP	ResNet-50, DeepLabv3+	Accuracy:0.9370, Sensitivity:96.67%, Specificity:99.15%, AUC:0.9980, F1 > 0.8, Kappa:0.9651
Li et al. (2022)	China	Pathologic Myopia, Myopic Maculopathy, Tessellated Fundus	Detection, Classification	57.148 images	CFP	DCNN-DS, EfficientNet-B0	**Internal testing:** Accuracy:96.5%, Kappa:0.922, AUC for PM:0.997, AUC for TF:0.985 **External testing (SDEH Dataset):** **PM:** Sensitivity:93.3%, Specificity:99.6%, AUC:0.998 **TF:** Sensitivity:98.8%, Specificity:95.6%, AUC:0.986 **External testing (QDEH Dataset):** **PM:** Sensitivity:91.0%, Specificity:98.7%, AUC:0.994 **TF:** Sensitivity:92.8%, Specificity:94.1%, AUC:0.970

Mao et al. (2023)	China	High Myopia, Myopic Maculopathy	Grading, Analysis of vascular morphological characteristics in high myopia	421 eyes	UWF	Transfer learning, RU-net	Accuracy:98.24%, Sensitivity:71.42%, Specificity:99.37%, Precision:73.68%, F1score:72.29
Wan et al. (2023)	China	Myopic Maculopathy	Diagnosis, Screening, Classification	1.750 images	CFP	VOLO-D2, EfficientNet V2, ResNet50	**VOLO-D2 model (best model):** Accuracy:96.60%, Kappa:95.60%
Zhu et al. (2023)	China	Myopic Maculopathy	Classification	4.252 images	CFP	Alfa-Mix+ Algorithm, Efficient Former, ResNet18, DenseNet169	**Efficient Former + ALFA-Mix+ (best model):** Accuracy:0.8964, Sensitivity:0.8643, Specificity:0.9721, Kappa:0.8537
Zheng et al. (2024)	China	Myopic Maculopathy	Diagnosis, Grading	1.199 images	CFP	Efficient Net (B0/B7), VGG16, ResNet50	**EfficientNet-B0 (best model):** Accuracy:88.32%, Kappa:83.58%
Chen et al. (2024)	China	Myopic Macular Degeneration	Prognosis, Progression	660 images (internal dataset) 212 images (external dataset)	CFP, SS-OCT	XGBoost	**Internal validation dataset:** Accuracy:0.84 ± 0.01, Sensitivity:0.83 ± 0.02, Specificity:0.85 ± 0.01, F1 Score:0.84 ± 0.01, AUROC:0.84 ± 0.006, AUPRC:0.87 ± 0.007 **External validation dataset:** Accuracy:0.80 ± 0.01, Sensitivity:0.97 ± 0.01, Specificity:0.63 ± 0.03, F1 Score:0.83 ± 0.01, AUROC:0.80 ± 0.008, AUPRC:0.83 ± 0.01

iii) Description and Commentary of the Studies Selected

The study conducted by Ran Du et al. in 2022 was built on 9.176 swept-source OCT images collected between the timeframe October 2015 and March 2019 from patients with high myopia registered in the Advanced Clinical Center for Myopia in Tokyo. The scientists carried out their research through monitoring with periodic follow-up examinations a total of 1.327 cases (2.400 highly myopic eyes, with mean axial length close to 29.5 mm) whereas the ultimate purpose of the study was to develop a deep learning algorithm via training soft labels models with the aim of minimizing physicians' uncertainty in diagnosing myopic maculopathy lesions. Nevertheless, the primary goal of the study was to compare and assess the differences between hard labels and soft labels in identifying myopic retinopathy through OCT images analysis, but also estimate the gap between human grading and these models in forecasting and classifying the disease. In total, 21 experts in myopia were involved in the research that examined the images for the presence of myopic neo-vascularization (MNV), myopic traction maculopathy (MTM) and dome-shaped macula (DSM), which are the

most common alterations and the main reasons for vision deterioration in pathologic myopia eyes. After the images' gathering and specialists' assessment was completed, the stage of data processing followed. Model construction was divided into hard labels and soft labels, the first obeying the principle of majority overshadowing minority regarding the diagnosis results whereas the second following the idea of converting the labels into probabilities (calculation of possibility between different grading results). The training neural network used in the algorithms' construction was Darknet-19. As a final step, model performance evaluation was held using statistical metrics such as kappa value (0.83 for myopic maculopathy, with $P<0.01$). In comparison to the rest of clinical entities examined, myopic traction maculopathy models (soft labels) presented a higher specificity and an area under the precision-recall curve (AUPR) greater than 0.876, with calculation of an area under the curve (AUC) close to 0.946. The DSM model achieved an AUC of 0.978 and AUPR of 0.653, whereas the MNV model achieved an AUC of 0.985 and AUPR 0.908. Lastly, a remarkable finding of the study was extracted by the final comparison of the results between the artificial intelligent models and the human graders. At first glance, the two methods showed similar consistency but after a more thorough examination models trained by soft labels presented a slightly higher level of certainty compared to those trained by hard labels in MTM identification, whose uncertainty level was more approximate to that of the physicians. This conclusion was drawn using kappa value as a calculation metric and the following diagram (Figure 14) reveals that the use of soft labels can indeed facilitate the screening of the disease in everyday clinical practice (Du et al., 2022).

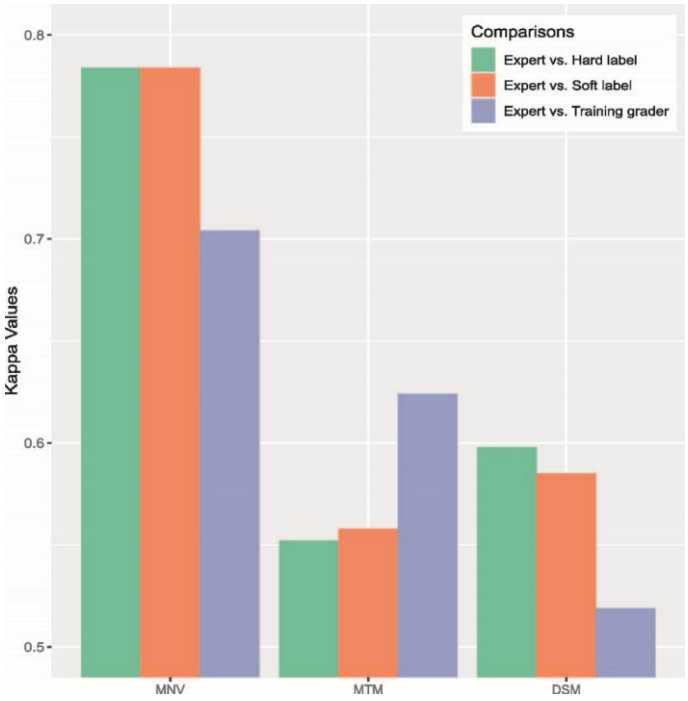

Figure 14: *Comparisons based on kappa value calculations among models and human myopia specialists regarding the three entities included in the study (Du et al., 2022).*

Another unique point of this research that needs to be underlined is that in real life conditions, experts are often obliged to examine more than one OCT image to extract a definite diagnosis result regarding the entities mentioned before (MTM, MNV, DSM), since exact differentiation between them is not always achieved with a single scan evaluation. As a result, their final decision may adopt the vague outline of probabilities, instead of a definite final answer, undermining in this way timely intervention in the emergence of sight- threatening complications. On the other hand, deep learning methodologies are built on the opposite logic of categorizing diseases into discriminate groups, thus providing an effective means of diminishing this ambiguity. Therefore, the innovative perspectives proposed by the authors (hard labels and soft labels) constitute a thorough attempt to clarify/resolve the uncertainty behind each individual diagnosis via discovering soft labels' potential in mimicking real life scenarios and by confirming their superiority in drawing more accurate diagnostic results. Finally, two important advantages of the studies worth mentioning are the following: a) effectiveness of the models trained by soft labels in incorporating the scientists' uncertainty during the conclusions drawing process, improving in this manner performance in image recognition by creating a simulation of real-life conditions on

OCT scans decoding, and b) utilization of a hospital-based database that contributed to the generalizability of the study carried out (Du et al., 2022).

During the previous year (2021), a retrospective/ multicohort analysis was carried out by Tien-En Tan et al. in Singapore who used a larger stock of retinal fundus photographs (226.686 images) to develop a deep learning algorithm for effective identification, risk stratification and screening of myopic macular degeneration cases. The primary internal validation of the algorithms was executed on datasets from Singapore, whereas the external testing was conducted on datasets from China, Taiwan, India, Russia and the UK. The researchers classified myopic maculopathy lesions according to the META-PM grading system and generated a deep learning algorithm on a second level using ResNet-101 as a convolutional neural network (CNN) to detect eyes with myopic macular degeneration. The scientists applied the gradient × input method to form heatmaps as a reference point for localization of lesions in positive cases. Finally, the performance of the deep learning algorithms for myopic maculopathy detection was compared against six specialists (retinal experts and ophthalmologists) on a small number (200 samples) of randomly selected retinal images among those examined. Regarding the statistical analysis parameters, the scientists calculated the area under the receiver operating characteristic (ROC) curve (AUC) to derive results on sensitivity and specificity of the study. The algorithm showed high efficiency (robust performance) in identifying myopic macular degeneration, with AUC more than 0.96, sensitivity more than 91% and specificity more than 85% across all datasets. Lastly, the algorithm's capability overpassed six human expert graders in the detection of myopic maculopathy, achieving similar error rates (97.5% sensitivity for myopic macular degeneration on external testing). The innovative implementation of a blockchain enabled AI platform allowed secure reporting of results for validation purposes, as well as data handling and sharing across three different sites in two countries (Singapore and China). The discoveries mentioned above indicate that the artificial intelligence- based models described could theoretically substitute human potential, providing an automated screening tool and an effective alternative solution in the identification of cases at highest risk for sight-threatening future complications. This intervention may prove to be timely given the global burden of myopia lurking on

the horizon (prediction for high prevalence of myopic cases worldwide), contributing to the reduction of workload regarding patients' first screening (Tan et al., 2021).

A more recent study published in June 2024 was written by Yanping Chen et al. and took place in the Zhongshan Ophthalmic Center in China. Its purpose was to forecast myopic maculopathy's progression via developing and validating an interpretable machine learning algorithm. In total, 660 patients with high myopia were included in the research which were followed up for 10.9 years on average. Between them, a relatively low percentage (20.2%, 133 cases) exhibited evolution of the disease in the following manners: newly-emerging alterations (51.9%, 69 cases), arising of patchy atrophy out of diffuse atrophy (8.3%, 11 cases), spreading of lesions (40.6%, 54 cases) and reporting of plus signs' development (6.8%, 9 cases). During the monitoring period, a series of retinal images were gathered by the patients examined that allowed determination of progression patterns of the disease and formation of a risk assessment system. Two ophthalmologists and one retinal specialist graded fundus photographs captured according to the META-PM classification system, whereas OCT imaging served as an auxiliary tool in case of suspicion of neovascularization development (CNV) in color fundus images. The Machine Learning Algorithms applied to perform the investigation were indicatively: XG Boost, logistic regression, random forest, Light GBM and neural network. Among them, the XG Boost algorithm presented the highest detection capability with an accuracy close to 0.85, sensitivity of 0.86, specificity 0.83 and F1 score approximately 0.85; measurements that confirm the superiority of the model. This model also demonstrated superior calibration ability compared with the others in forecasting myopic maculopathy progression. These systems were used to derive meaningful information regarding myopic macular degeneration progression via calculating the average performance of each modality. After the validation phase of the models (in an internal dataset and an external cohort for further evaluation of their generalizability) was completed, statistical analysis was conducted via comparisons with t-tests and Mann-Whitney tests measurements for continuous data or chi-square tests and Fisher exact tests measurements for categorical data. As a fact, a P-value less than 0.05 was statistically significant. To summarize, this study is based on long-term data and observations to predict MMD progression over a decade in high myopia cases. The methodology unfolded via these

algorithms' deployment displayed high accuracy and robust clinical value in estimating future MMD traits. A major finding that must be highlighted is that the sub foveal choroidal thickness (SBCT) parameter that derives from SS-OCT calculations is the most variable factor for forecasting evolution of the disease. A satisfactory explanation to this phenomenon could be that prolonged choroidal ischemia due to increased axial length contributes to myopic maculopathy development. Another point that must be highlighted is the unique characteristic of the study to include a wide range of ages, permitting detecting the sight-threatening complications of the disease in younger age groups (e.g., adolescents). It is an element that holds precious clinical value given the rapid progression of the disease in this group of patients and emphasizes the need for early screening and intervention in a primary stage to avoid dangerous complications. The arguments above confirm and reinforce the urgency for identification of changes on a first scale to ensure maximum healthcare benefits for this vulnerable population category (Chen et al. 2024).

Looking back a year ago, we discover the study conducted by Jiabao Mao et al. in 2023 after recruiting 203 subjects (317 eyes with high myopia examined) during July 2020 and January 2021 for evaluation at the Eye Hospital of Wenzhou Medical University in China. The analysis was based on UWF retinal imaging examination (green laser images) and the parameters measured were vessel angle, fractal dimension, vascular density and number of vascular branches. The research included 61 healthy control subjects (104 normal eyes examined) to carry out comparisons. Firstly, the images were classified into five categories (C0-C4) according to the META-PM grading system and then transfer learning technology (RU-net network) was used to depict retinal vessels fundus distribution in different degrees of high myopia samples. Secondly, statistical analysis calculations were made and correlations regarding axial length, BCVA, age and vascular characteristics were performed with the assistance of Pearson tests ($P<0.05$), whereas paired samples were evaluated with t-tests application. Segmentation analysis of UWF images in collaboration with a deep learning system utilization, exhibited satisfactory performance metrics with an accuracy of 98.24%, sensitivity of 71.42%, specificity of 99.37% and precision of 73.68%. Along with the disease's evolution (increased severity of myopic maculopathy

and eyeball elongation), vessel density and angles decreased, and fewer vascular branches were noted (these differences were also observed in comparison with healthy individuals, and they constitute statistically significant measurements, P<0.001). Lastly, an association pattern between these retinal vascular morphology parameters and age (older), BCVA (worse) and axial length (longer) was observed (Mao et al., 2023).

During the same year, Cheng Wan et al. proposed a myopic maculopathy grading model for automatic screening of lesions through examining a satisfactory number of retinal fundus images (1750 photographs). The five-category models were trained with Vision Out Looker for Visual Recognition (VOLO), EfficientNetV2, and ResNet50. Among the large amount of color fundus images initially gathered from the Eye Hospital of Nanjing Medical University, 174 fundus images were finally chosen for external testing. The diagnostic results were assessed using evaluation metrics such as sensitivity, specificity, negative predictive value (NPV), positive predictive value (PPV), area under the curve (AUC), kappa value, accuracy, and receiver operating characteristic curve (ROC curve).

The accuracy of the VOLO-D2 model was measured to be 96.60% with a kappa value of 95.60%, proving its effectiveness in identifying pathological macular lesions. For the diagnosis of images classified as C0 (absence of myopic lesions) the model achieved a performance of 100% in all metrics. Regarding leopard appearance of the fundus (C1), the model's sensitivity (SE) reached the percentage of 96.43%, NPV was 98.33%, whereas specificity and PPV were rendered with the highest ranking of 100%. As for diffuse chorio-retinal atrophy subgroup (C2), the following metrics were recorded: AUC 97.73%, SE 96.88%, SP 98.59%, PPV 93.94% and NPV 99.29%. Relatively similar measurements (but a little lower) were observed for categories C3 (patchy chorio-retinal atrophy) and C4 (macular atrophy), with a performance of 100% (sensitivity) and 98.10% (specificity) for the last one. Additionally, the scientists generated maps that were based on gradient-weighted class activation (Grad-CAM) to visualize the diagnosis extracted by the VOLO-D2 model regarding myopic maculopathy lesions recognition (Figure 15).

EfficientNetV2-S demonstrated a relatively lower performance in the diagnosis of all categories, with a sensitivity >89% and a higher consistency rate. Finally, the ResNet50 model achieved low sensitivity in macular atrophy identification and scored better results in non-myopic retinal degenerative and leopard fundus lesions. Based on the statistics above, these models can prove to be useful tools in the initial automatic screening of myopic maculopathy lesions (Wan et al., 2023).

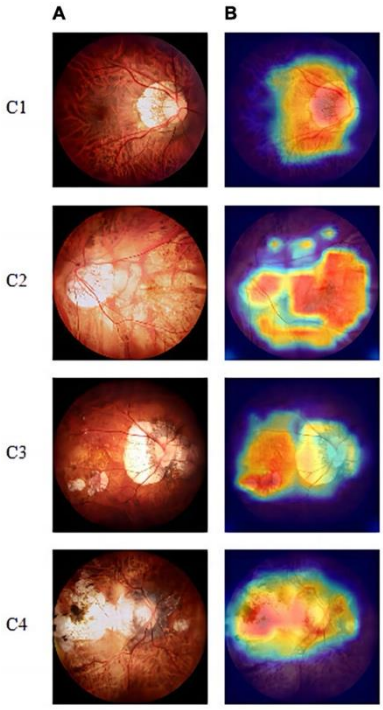

Figure 15: *Visualization-based diagnosis by the VOLO-D2 model. (A) Original image. (B) Grad-CAM. Grad-CAM shows that the model focused on the myopic maculopathy area. From left to right, we can see the original fundus images of the four lesions along with the corresponding gradient activation heat maps. Grad-CAM, gradient-weighted class activation mapping.*

Two other studies worth mentioning are the following. First, the Bo Zheng et al.'s study in 2024 in Shenzhen Eye Hospital, China who assessed 1.199 color fundus photographs to develop a myopic maculopathy grading method using deep learning methods (EfficientNet-B0) and struggle with the problem of delayed diagnosis and classification of different myopic maculopathy categories. The application of this AI scaling method facilitated the identification and distinguishing between the different degrees of myopic maculopathy and normal fundus images (Figure 16).

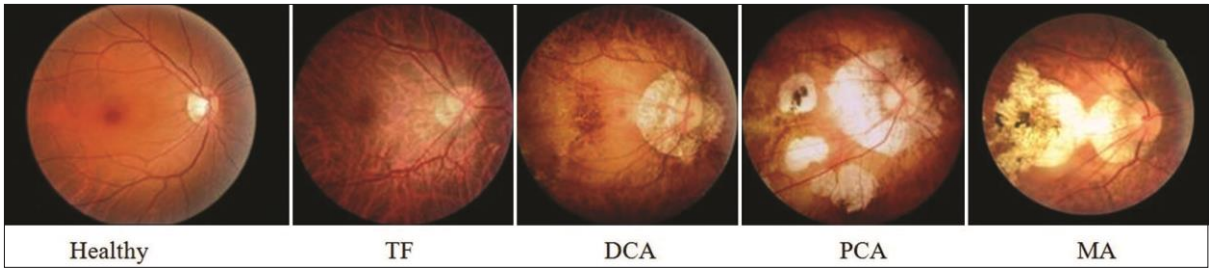

Figure 16: *Images of a normal fundus and four stages of myopic maculopathy progression-tessellated fundus, diffuse and patchy chorio-retinal atrophy, macular atrophy (Zheng et al., 2024).*

Accurate diagnostic results of the disease were obtained through examination of the photographs by two ophthalmologists, but the contribution of a third specialist was mandatory in case of uncertainty. SPSS statistics were used to derive conclusions regarding the sensitivity of the model for tessellated fundus (96.86%), diffuse chorio-retinal atrophy (75.98%), patchy chorio-retinal atrophy (64.67%) and macular atrophy (88.75%). The specificity measurement for all four types of myopic macular degeneration was >93%. The kappa-value of the EfficientNet-B0 model was calculated to be close to 84%, an indicator of a strong diagnostic consistency. This study also trained Efficient-B1 to B7, VGG16 and ResNet50 models, which demonstrated lower diagnostic results compared to the EfficientNet-B0 model. It must be noted that all different types of models achieved 100% accuracy in diagnosing healthy color fundus photographs. In total, ten separate AI-models (EfficientNet-B0-B7, VGG16 and ResNet50) were used to extract evaluation index results concerning the disease's classification. As a next step, ROC curves were created to assess the performance of the proposed classification model. Figure 17 illustrates the ROC curves of the normal fundus, and the four degrees of myopic maculopathy diagnosed with the assistance of the ten models mentioned before. These curves represent an alternation between the true-positive rate (TPR, sensitivity) and the false-positive rate (FPR) across different classification thresholds. The area under the curve (AUC) constitutes a brief calculation of the model's overall performance. The ideal formation of a ROC curve should have a proximity to the top left corner in the diagram, displaying high TPR (accuracy index) and low FPR (error rate index).

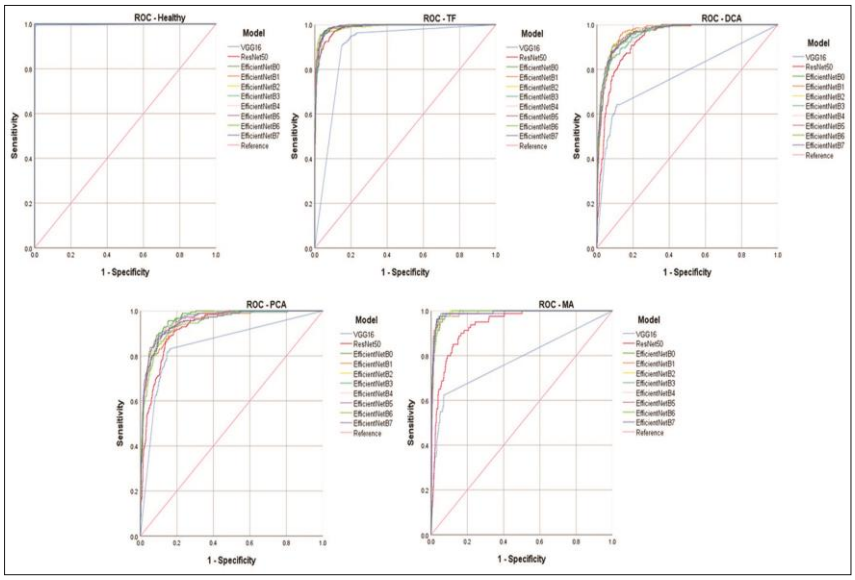

Figure 17: *ROC curves of the ten models for five myopic maculopathy degrees (healthy, TF, DCA, PCA, MA) (Zheng et al., 2024).*

Based on these observations, the researchers arrived at the conclusion that the preliminary screening of myopic maculopathy by applying the algorithms above can result in an effective scaling system for disease's classification, improving responsiveness and delaying vision impairment in these patients. The Efficient Net-based myopic maculopathy grading models demonstrated high sensitivity and specificity in diagnosing the disease's progression by recognizing healthy fundus and four types of myopic maculopathy in color fundus photographs. Finally, the design of ROC curves reveals better results for normal fundus identification and lower diagnostic ability in the category of patchy chorio-retinal atrophy (Zheng et al., 2024).

The year before (2023), Shao-Jun Zhu et al. run simulations on classifying high myopic maculopathy lesions with the use of advanced deep learning models and a complete training set of 4.252 images. The primary aim of the study was to optimize the ALFA-Mix active learning algorithm and achieve superior grading results and enhanced model performance by combining it to Efficient Former (an effective solution when labeled data is limited). A brief description of the model's operation is as follows: in the first stage feature extraction takes place from unlabeled and labeled images, which are then mixed to elicit predictions. In the second stage, the algorithm identifies the

most representative samples with high information content and submits them to experts for annotation. In this manner, the cost required for expert annotation in a large dataset is reduced, maintaining high accuracy levels. This combination reached high evaluation metrics with an accuracy of 0.8964, sensitivity of 0.8643, specificity of 0.9721 and kappa value of 0.8537. The scientists introduced with their investigations an innovative approach that offers a convenient alternative in the analysis and diagnosis of high myopic maculopathy cases. This is mainly due to the algorithm's ability to find the golden ratio between uncertainty and variability, improving disease classification accuracy. A representative confusion matrix (visualization method for classifying algorithm's results) is depicted on Table 3 (Zhu et al., 2023).

Table 3: *Confusion matrix of ALFA-Mix + algorithm after combining it with Efficient Former for enhanced results (Zhu et al., 2023).*

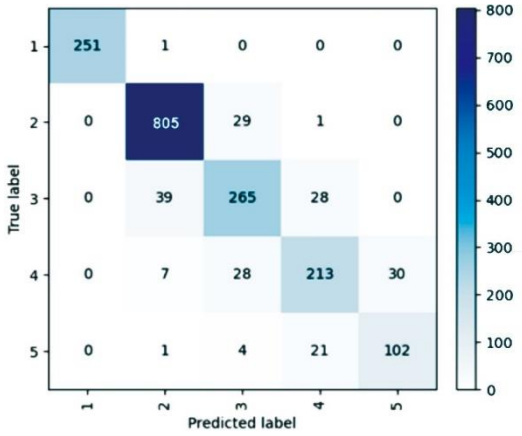

A flashback of two years leads us to the discovery of three studies conducted during 2021, in China. The first one was carried out by Li Lu et al. in 2021 who analyzed the development of an AI-Model based on deep learning algorithms for identification of myopic maculopathy lesions in retinal fundus photographs. The methodology followed included 32.010 color retinal fundus images that were graded for training and cross validation according to the META-PM classification system. This large stock of records was collected between July 2016 and January 2020 from the First Affiliated Hospital of School of Medicine, Zhejiang University. Before the image analysis process, the scientists defined, annotated and set a reference standard, deciding that fundus

images of category 2 (diffuse chorio-retinal atrophy) or worse that exhibited at least one of the “Plus” lesions were considered to have pathologic myopia. A total of 20 ophthalmologists from three ophthalmic centers that achieved a kappa value ≥0.81 were selected to manually grade and annotate the images. The experts were separated into five groups (one senior specialist at each group) and the diagnoses that gained a unanimous vote by three graders of each team were set as the reference standard. After the gradable images were determined, algorithm I was generated according to the presence of pathologic myopia in each eye. On a second level, the gradable images were rendered a myopic maculopathy label category, a procedure that led to algorithm II creation. On a third level, experts localized “Plus” lesions within the image by drawing boxes and formed in this way algorithm III. These three algorithms were used to develop two AI models (I & II); the first one contained Algorithm I and distinguished between non pathologic myopia and pathologic myopia images, and the second consisted of Algorithm II, III and a logical analysis module based on META-PM classification. Lastly, comparison of their performances took place to obtain an optimized model for PM identification.

Algorithms I and II were composed of a CNN architecture named ResNet18, whereas Algorithm’s III construction was based on a feature Pyramid network (FPN), that contained faster region-based CNN. The scientists executed external validation and expert-machine comparisons to assess the algorithms’ effectiveness more thoroughly and with this aim they recruited 1000 images from three separate hospitals in Zhejiang Province. The images in the external validation dataset were simultaneously graded by the algorithms and two experts that did not participate in previous grading. Their comparison results served as tools for further performance quantification. The images misclassified by Algorithms I and II were further analyzed by a senior retinal specialist. A convolutional visualization layer was implanted at the end of Algorithm II that generated a heatmap and highlighted the strongly predictive regions on retinal fundus images. The following indexes were used to evaluate the algorithm’s performance: AUC (0.995), Accuracy (0.973), Specificity (0.981), Sensitivity (0.939) for algorithm I, and macro-AUC (0.979), Accuracy (0.967) and Quadratic-weighted kappa (0.988) for algorithm II. Algorithm III achieved an accuracy of 0.970 to 0.994 for recognizing plus lesions and an F1 score of 0.685 to 0.889 for identifying and localizing myopic

maculopathy lesions. A photographic representation of algorithm II ability in grading myopic maculopathy stages is provided in Figure 18 via a heatmap feature analysis.

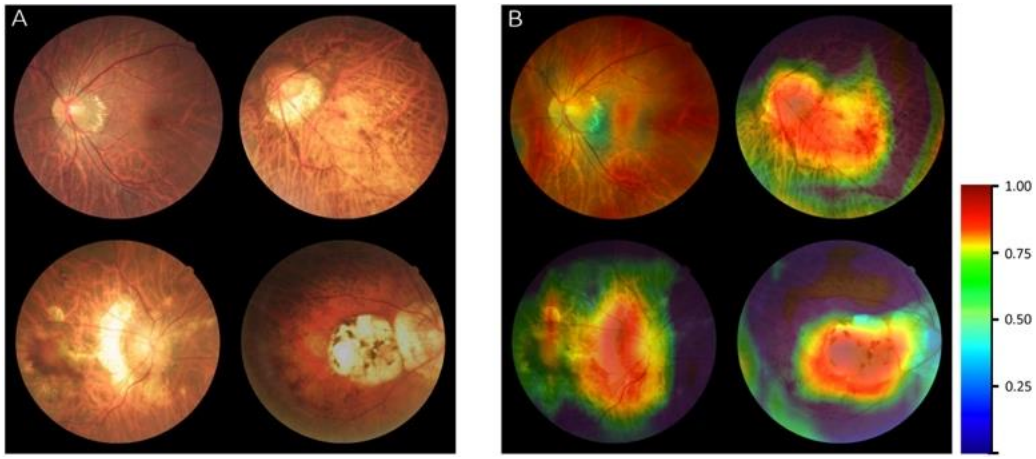

Figure 18: *Visualization of algorithm II for classifying the category of myopic maculopathy (MM). (A) The original images of different MM (Category 1–Category 4). (B) Heatmap generated from deep features overlaid on the original images. The typical MM lesions were observed in the hot regions.*

External validation contributed to the drawing of the following conclusions: a significant difference was observed between AI models and experts in identifying PM (P=0.013), but also in distinguishing different MM lesions (P<0.001). Nevertheless, the performance of the deep learning algorithms was almost equal to that of the experts. For instance, regarding PM identification, model-2 exhibited higher accuracy than the general ophthalmologist (96.9% vs 96.1%), whereas for Algorithm II and III the difference gap was within the spectrum of 3% (Figure 19). These statistical measurements confirm that the proposed AI models demonstrate satisfactory performance in a real world setting and the algorithms' application can facilitate diagnosis and screening in pathologic myopia patients on a large scale in the future (Lu et al., 2021).

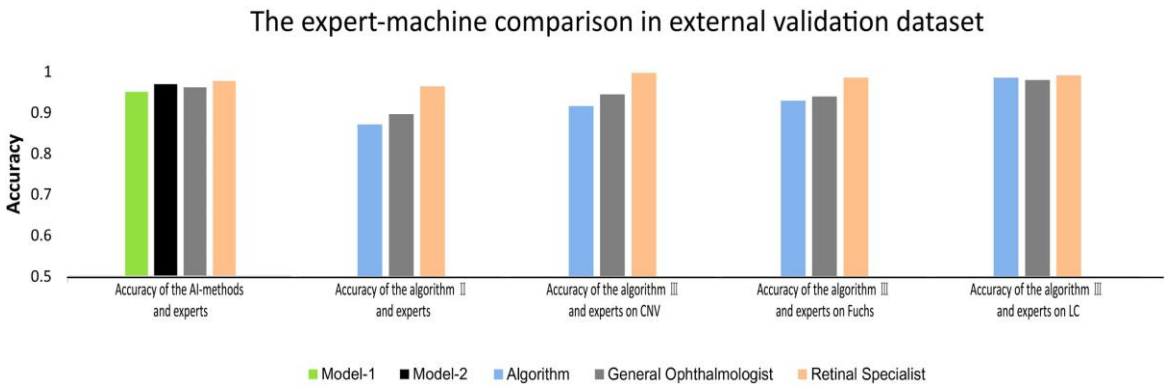

Figure 19: *The comparison between deep learning algorithms/AI-models and experts on accuracy in external validation (Lu et al., 2021).*

The next study conducted during the year 2021 worth to be cited was the research product of a scientific team made up of Xin Ye et al. that collaborated in the School of Ophthalmology and Eye Hospital in Wenzhou Medical University. The purpose of this investigation was to engineer a deep learning system using Optical Coherence Tomography Images that can automatically screen and identify myopic maculopathy lesions. This AI model was developed with the aid of 2.342 OCT macular images acquired from 1041 high myopia patients admitted to the Eye Hospital of Wenzhou Medical University from May 2016 to May 2020. The scientists trained five models that implemented ResNeSt101 architecture to distinguish the following features: macular Bruch membrane (BM) defects, macular choroidal thinning, subretinal hyperreflective material, myopic traction maculopathy and dome-shaped macula. With the aim of corresponding the AI system applied in real-world conditions, 450 images from 297 high myopia patients were chosen as an independent test dataset used for validation purposes. Each diagnosis was made via mutual consultation between two retina specialists and two ophthalmologists. The statistical analysis results for performance quantification regarding myopic maculopathy identification included an AUC measurement of ROC curves between 0.927 and 0.974 and sensitivity measurement equal to or greater than this of junior retinal specialists (56.16-99.73%). A heatmap illustration of these interpretations and a brief explanation of the AI system's workflow is depicted below (Figure 20).

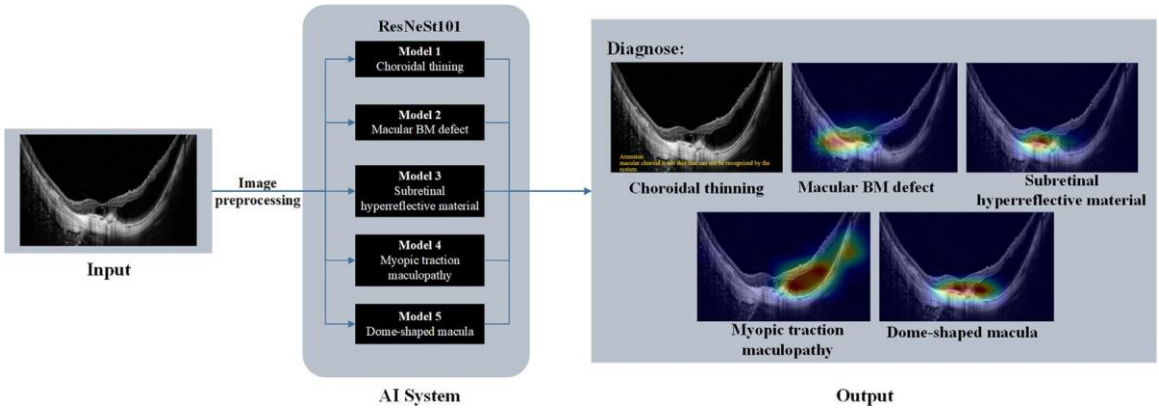

Figure 20: *Workflow schematic representation of the AI system deployed by the scientists (Ye et al., 2021).*

The final step of the research consisted of comparisons between the AI models and human retinal specialists. Each of the expert's diagnosis was compared to a gold standard to evaluate the AI system performance. For myopic traction maculopathy sensitivity of the AI system was calculated to be 92.80% and specificity 90.50%, whereas the corresponding metrics for junior specialists' assessment were: sensitivity 89.37% and specificity 90.98%, and for senior specialists: 97.71% sensitivity and 96.93% specificity. Heatmaps were created not only for myopic maculopathy identification but also for macular Bruch membrane defects (hallmarks of myopic CNV related macular atrophy and patchy atrophy, indicating absence of photoreceptors and lower visual acuity) and choroidal thinning that plays a pathogenetic role in the progression from normal fundus to diffuse atrophy (Figure 21, 22).

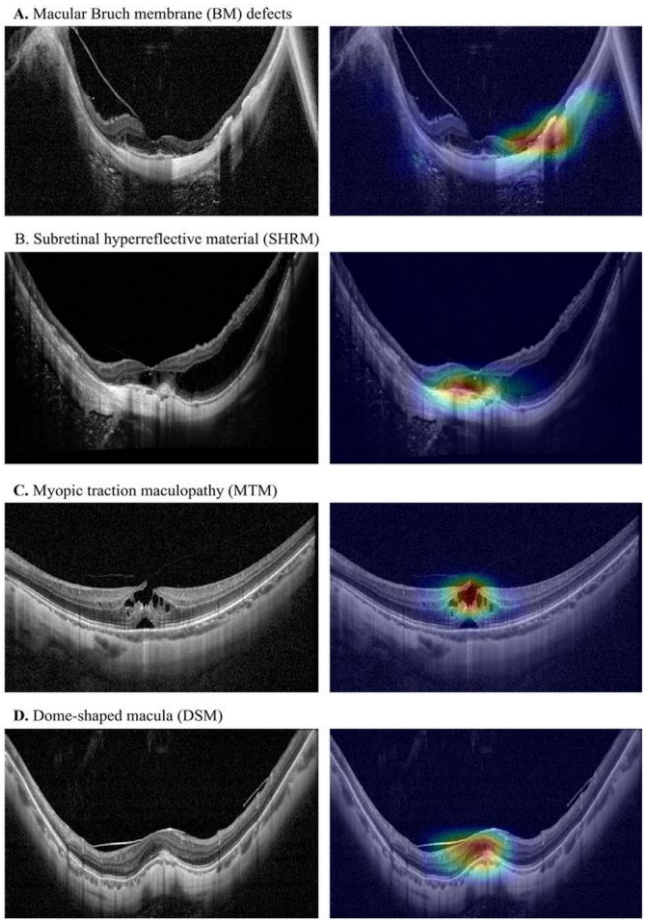

Figure 21: *Heatmaps illustration of the five different conditions examined by the scientists' investigation (Ye et al., 2021).*

To summarize, the deep learning algorithm used by the researchers for the diagnosis and grading of myopic maculopathy was constructed based on a convolutional neural network (CNN) architecture and achieved equal or better results than those of junior retinal specialists, since senior retinal specialists' assessments maintained higher diagnostic levels (Ye et al., 2021).

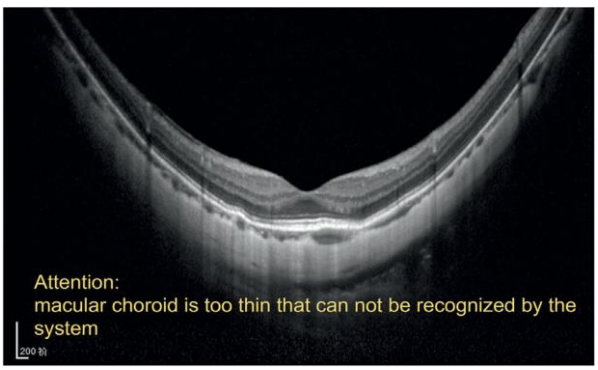

Figure 22: *Measurement of sub foveal choroidal thinning (less than 62 μm) using an AI system (Ye et al., 2021).*

The next study conducted in 2021 that must be commented on in this review was carried out by Yuchen Du et al. and examined 313 patients (457 eyes), that were all over 50 years of age and had an axial length more than 26 mm. They were separated into a severe and non-severe myopic maculopathy group. Radiomics analysis method was applied to identify features of the severe myopic maculopathy condition from the optic disc region. ROC curves were used as a measure of their performance in classifying the severe stage of the disease. The methodology consisted of the following elements: 1. Delineation of the regions of interests (ROIs); 2. Construction of a feature pool using an automatic extraction strategy and 3. Selection of discriminative features with the aid of correlation analysis and machine learning algorithm. The performance of new image features' set in classifying severe MM was scored as 0.8263 AUC on the validation dataset, whereas the performance of the clinic feature set was scored as 0.7925 AUC. The two categories were merged to form a union feature set that gained the number of 0.8358 on validation dataset. The main findings of the research executed were the following: a) eight new images features were determined to show greater ability (higher overall performance) than clinic features in identifying severe myopic maculopathy cases. b) an effective machine learning tool to extract and decipher various MM-related image features in an automatic manner was exploited; and c) deviations between PDCA and MDCA were confirmed by both new image and clinic features. This discovery unraveled a more comprehensive view regarding the characteristics' development and progression patterns of myopic maculopathy lesions. This research presents a unique perspective that could function as a substitute for the subjective evaluation of different myopic maculopathy graders (Du et al., 2021).

Continuing, He X. et al. during July 2022 used deep learning (DL) methodologies that were based on transfer learning (TL) to formulate an automated AI grading system that could recognize different stages of myopic maculopathy guided by OCT images results. The scientists conducted a retrospective study by exploiting a stock of 3.400 macular OCT photographs acquired from 2.866 myopic patients. The ATN classification system functioned as leverage for the development and training of two separate Algorithms (A & B). Although both served to identify targeted MM lesions,

Algorithm B included the complementary element of transfer learning (TL) and therefore demonstrated higher performance with a macro-AUC calculation of 0.986, accuracy of 96.4% and kappa-value of 0.986. In the test dataset, the algorithm achieved an AUC of 0.986, an accuracy of 96.04%, and a quadratic-weighted kappa of 0.940. On the external validation dataset, its performance remained strong, with an AUC of 0.938, an accuracy of 90.6%, and a quadratic-weighted kappa of 0.897. As far as human- machine comparison testing is concerned, the algorithms' results appeared to be inferior to retinal specialists but equal to ordinary ophthalmologists in recognizing various posterior pole alterations. Res Net-18 architecture was unraveled to derive meaningful output information on macular schisis recognition as represented in the diagram below (Figure 23). Finally, visual heatmap analysis of Algorithm B was carried out that highlighted with hot colors the most determining areas for classification of the disease on the original image (He et al., 2022).

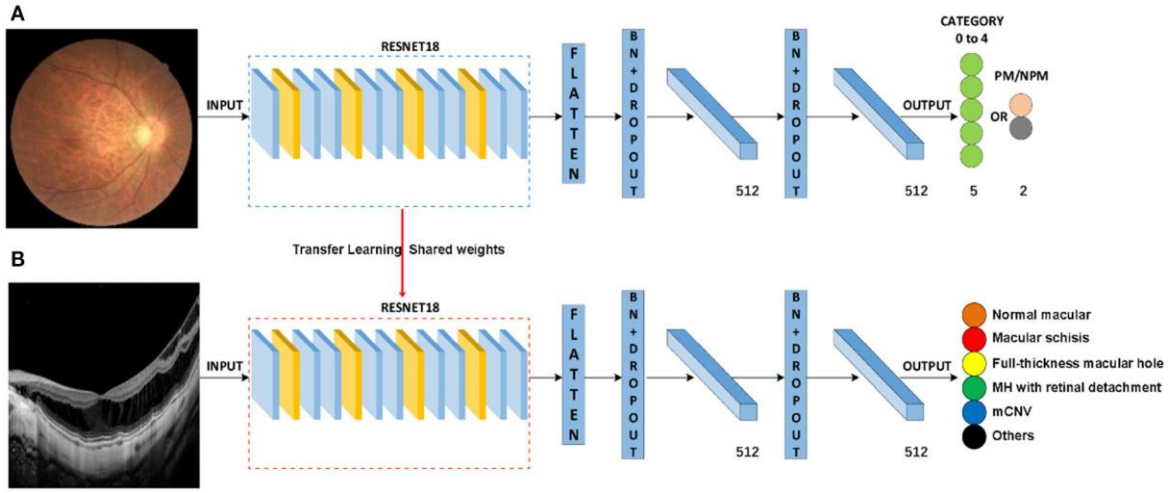

Figure 23: *Schematic illustration of algorithm's deployment. OCT image grading methodology is based on Transfer Learning (He et al., 2022).*

To complete the analysis process, we will focus on two surveys that were based on Color Fundus Photographs and were published almost simultaneously (during the year 2022) by two different groups of experts. The first one was conducted by Tang J. et al., during April 2021 and focused on the construction of a DL model suitable for diagnosis, identification and segmentation of myopia-related lesions. Four specialists were assigned to annotate and classify the images with the use of DeepLabv3+ and ResNet-50 network respectively. On the next scale, the two models were combined to

generate an integrated co-decision system for classification and segmentation analysis. In total, 1395 CFPs were gathered from 895 patients, whereas the final statistical measurements for evaluation of the model were: accuracy of 0.9370, quadratic-weighted κ coefficient of 0.9651 and AUC of 0.9980 in diagnosing pathologic myopia. These findings (demonstration of sufficient performance results) translate into the assumption that the application of the aforementioned automated techniques could successfully not only grade and diagnose but also monitor and follow-up advancement of the disease's alterations on a clinical level, facilitating the task of ophthalmologists (Tang et al., 2022).

The second study worth commenting on was conducted by Li J. et al. during the same year (2022) and used a deep convolutional neural network (DCNN) system to recognize absence of myopic maculopathy (MM), tessellated fundus (TF) and Pathologic Myopia (PM). An amount of 57.148 images were graded by four ophthalmologists and analyzed using internal and external datasets to evaluate the model's performance. The system achieved its best performance metrics in the **SDEH dataset** with a sensitivity of 93.3%, specificity of 99.6% and AUC of 0.998 for PM recognition, whereas the corresponding measurements for TF identification were 98.8% for sensitivity, 95.6% for specificity and 0.986 for AUC parameter. These numbers confirm the system's robust potential in differentiating a variety of myopic maculopathy lesions on a large scale and significantly raise the probabilities for a real-life application of this innovative approach in the next decades (Li & Wang et al., 2022).

iv) Discussion

The analysis of the selected studies provides valuable information regarding the reliability and usefulness of each investigation. An initial review reveals that studies that included a higher amount of OCT or CFP images were more suitable for the classification, diagnosis and risk assessment of the disease's evolution compared to those that were built on a smaller amount of data. This gathering of a larger volume of photographs increases the generalizability of the study and ensures its validity and diversity, leading to improved performance results. Indeed, AI models developed by

researchers such as Du et al. (2022), Tan et al., He et al., Zhu et al., Lu et al., Ye et al., who utilized extensive datasets, demonstrated superior performance across parameters such as sensitivity, specificity, accuracy, AUC, and kappa-value. In contrast, studies conducted by Chen et al., and Du et al. (2021), which were based on smaller datasets, exhibited relatively lower performance metrics.

Continuing, the research conducted by Mao et al. introduced the special feature of utilizing more advanced techniques (317 Ultra-Wide Field Images gathered during July 2020 and January 2021) and presented the highest accuracy (98.24%) and specificity (99.37%) measurements in relation to the studies cited before, with the drawback of achieving lower sensitivity (71.42%), precision (73.68%) and F1 score (72.29%) results. Moreover, the use of OCT imaging has been shown to be a more accurate diagnostic instrument that allows precise assessment of disease's progression compared to Color Fundus Photography. Nevertheless, it does not constitute the first-choice examination on the screening of these patients since it is more time-consuming and expensive. This observation brings to the surface the need to exploit multimodal imaging (Color Fundus Imaging, OCT imaging and Ultra-Wide Field Photography) to function cooperatively in clinical settings for future studies. This proposal will prospectively accomplish a more complete approach and deeper understanding of myopic maculopathy, always including the catalytic role of artificial intelligence in this endeavor. Another critical point is the limited nationality range (selection of patients from the Chinese population) that constitutes a common element in all of the studies analyzed. As a result, the exclusion of other ethnicities limits the generalizability of results and detracts from the scalability of research on a Multinational and European level. Therefore, future involvement and funding of similar scientific research projects in populations of different countries will unfold the perspective of their potential application on a world-wide scale.

A key conclusion of the analysis is the comparison between human experts and AI in assessing myopic maculopathy lesions. Deep Learning Algorithms reached the levels of a general ophthalmologist in diagnosing the disease but maintained lower performance rates compared to senior retina specialists. This observation indicates that the construction of AI models based on deep learning is still at an experimental stage and needs further processing before reaching full autonomy and replacing the

clinical decisions made by experts in this field. However, their utility and helpful role in the initial screening of myopic maculopathy patients and the early detection of sight-threatening complications, such as glaucoma and myopic choroidal neovascularization, is widely acknowledged given the thorough review presented in Chapter III.

Another crucial aspect in the deployment of AI models for myopic maculopathy assessment is Explainability. The ability to interpret how AI arrives at its conclusions is fundamental for its acceptance in clinical practice. The explainable AI (XAI) techniques, such as Grad-CAM, and SHAP used in Ye et al., Wan et al., Chen et al. and other studies, enhance transparency by highlighting the most relevant regions in an image that contributes to the model's decision. This procedure fosters trust among ophthalmologists and enables validation and refinement of AI predictions, improving overall diagnostic reliability.

In general terms, the technology embodied in AI algorithms can optimize provision of accurate health care services, enhance scientific research on myopic maculopathy screening and identification, and offer a complementary advantage to human expertise. A supplementary element that could strengthen the system's complexity and improve its modernization index is the integration of additional information such as medical history, demographic data, comorbidities and genetic indicators of each examined case. This approach could signal a revolutionary phase in data accumulation, image decoding, initial screening and automatic identification of myopic maculopathy cases, always in cooperation with Artificial Intelligence Detection Systems. Finally, this innovation can optimize disease control strategies by adapting treatment guidelines to each patient's needs, facilitating in this manner effective monitoring of disease progression and upgrading an individual's quality of life on a broader scale.

v) Limitations of the Studies Analyzed

Each of these studies appeared with several limitations such as: restriction to Japanese population for the one conducted by Ran Du et al. in 2022 (absence of

application to other ethnicities for a more objective consideration), use of patients' images with prior vitreoretinal surgery, macular atrophy not examined, underdiagnosis of controversial cases and need for optimization of the threshold value to balance sensitivity and specificity. Also, the researchers included OCT images exclusively (no use of multimodal imaging) in their investigation that are often accompanied by artifacts in myopic maculopathy patients due to increased axial length. This generates errors and noise signals that alter image quality and influence the validity of grading results, thus hindering the effective diagnosis of the entity. The research conducted by Tian-En Tan et al. included the following drawbacks: detection of myopic macular degeneration as a binary (present or absent) result, not identifying the five categories of the META-PM classification system or individual plus lesions due to the small proportion of these images in the training dataset, narrow spectrum in the detection of myopic findings such as: optic nerve head tilt, peripapillary atrophy, posterior staphylomas and finally low image resolution leading to reduced performance and generalization ability of the algorithm. The investigation carried out by Yanping Chen et al. in 2024 using color fundus photographs of 660 patients presented the following limitations: external validation of the model was held in a separate Chinese cohort with a short follow-up period (4 years), lack of assessment of its generalizability to other ethnic groups apart from the Chinese population sample, influence of the COVID-19 pandemic in scheduling the visits for ophthalmological examination, not inclusion of genetic data in the analysis, utilization of the SS-OCT diagnostic tool alone (no SD-OCT assessment), insufficient depiction of posterior staphyloma using 45° fundus camera (limited imaging range), need for utilization of other imaging techniques for a more holistic evaluation and therefore a more precise diagnosis.

Continuing, the study published by Jiabao Mao et al. in 2023, that included ultrawide-field retinal fundus images of 421 eyes, was a single-centered, hospital-based research and a vague peripheral deformation of the photographs was noted. In addition, Cheng Wan et al. in 2023 used a moderate amount of data (1750 color fundus images) due to difficulty in collection, leading to an incorrect diagnosis of some lesions and highlighting the need for improvement in image segmentation methods. Xiaoying He et al. in 2022 evaluated a larger amount of OCT images (3.400 was the indicative number) to classify myopic maculopathy. Nevertheless, a low quality of the images captured was observed as well as a co-existence of multiple types of MTM in one

picture of each case. Yuchen Du et al. in 2021 explored the field of Pathologic Myopia to arrive in a myopic maculopathy classification (severe stage) using machine learning through analyzing 457 color fundus photographs. However, the absence of follow-up data for further testing of the hypothesis was a significant drawback of this study. The research carried out by Shao-Jun Zhu et al. in 2023 regarding the deployment of a grading system for high myopic maculopathy cases with the contribution of a deep learning algorithm and the utilization of a great amount of color retinal fundus images (4.252) exhibited limitations in the following domains: scalability, computational efficiency, image segmentation and quality of the samples used. Two years before (2021), Li Lu et al. examined a great amount of color retinal fundus images (32.010) to grade myopic maculopathy using convolutional neural networks (CNN) as a reference algorithm. Even though the model achieved satisfactory performance, the need for multimodal imaging (OCT, OCTA, MRI and FA) was emphasized for a more successful detection of posterior staphylomas and lacquer cracks. During the same year, Xin Ye et al. screened and classified 2.342 OCT images with the assistance of a Deep Learning Artificial Intelligence System that raised the following issues: miscalculation, low image quality, low accuracy, misdiagnosis, two medical centers involved (need for multicenter research). The next year (2022), Jia Tang et al. and Jun Li et al. focused their research on color fundus photographs analysis to diagnose myopic maculopathy via exploitation of Deep Learning Tools. Despite the algorithms' fulfillment in achieving adequate evaluation metrics, some of the indicative disadvantages of their studies are listed below: small quantity of images, reduced generalization ability of the model and absence of OCT imaging data in the case of the aforementioned authors and simplification of the META-PM classification system, absence of OCT and wide-field fundus imaging, lack of automatic image quality evaluation and assessment of clinical samples only (community population examples not included in investigation) as for the editors mentioned second. Finally, Zheng et al.'s research in 2024 on an AI-based myopic maculopathy grading method using Efficient- Net presented with the following limitations: no inclusion of OCT images that could offer more detailed information on anatomical structures of the macular region (collection of CFFs exclusively), since the combination of different imaging modalities could yield better results. Additionally, the models trained for recognition and diagnosis of the disease are challenging to apply in real-world settings, whereas restricted DCA

(diffuse chorio-retinal atrophy) and PCA (patchy chorio-retinal atrophy) data led to lower sensitivities of 75.98% and 64.67% respectively. These results are better suited for preliminary disease screening rather than substituting professional diagnosis made by specialists in this field.

Although XAI techniques help make AI decisions more understandable, they are not always reliable. The way AI highlights important features can be inconsistent, which may lead to confusion for doctors. More research is needed to make these explanations clearer and ensure they are truly helpful in medical practice.

The issue of cost- effectiveness should not be neglected, especially when it comes to the application of dual stream DCNN models as proposed by Li et al. in 2022, whose evaluation of feasibility in a real-world setting needs further investigation. In addition, the inclusion of the OCT imaging modality (especially enhanced depth imaging-EDI) that offers the supplementary advantage of fovea choroidal thickness calculation along with the basic fundus photograph examination is a crucial procedure that needs to be implemented on the first screening of these patients. On the other hand, the additional utilization of more advanced imaging techniques such as wide-field fundus imaging is imperative to permit assessment of the periphery of each highly myopic fundus and to primarily detect alterations attributed to increased axial length in this high-risk population. Lastly, an independent quality control check should be performed in each of the studies mentioned above, since the existence of ineligible images due to non-clear refractive media (e.g., cataract, prior vitreoretinal surgery) limits the statistical reliability of investigations. Finally, the observations cited above indicate that a more careful and rational selection of samples from the general population is necessary to improve the generalizability of the models exploited and thus increase the objectivity index of the studies examined. Following this direction, complementary collaboration between centers on a worldwide scale should be promoted to combat lack of diversity and achieve high-quality dataset collection amongst different population groups. Undoubtedly, ethical issues regarding transparency, human bias, data protection, decision making and liability need to be addressed, and global barriers must be crossed before the final legalization of the methodologies analyzed in the previous chapters. Despite these challenges, AI, ML and DL algorithms are aspired to have a significant clinical impact on myopic maculopathy recognition in the years to come.

D) CONCLUSION

The investigations conducted so far in this field show that AI-based models can be successfully applied to the first screening of myopic maculopathy patients on a large scale in the future, reducing the workload of ophthalmologists and improving the techniques of immediate intervention when major, sight-threatening complications arise. Nevertheless, the question of whether experts' evaluation and critical thinking can be replaced by automated analysis techniques remains unanswered, since it constitutes a controversial issue that requires extensive discussion to be resolved. In every situation, the studies mentioned above prove that the application of deep learning and machine learning methodologies that are based on the construction of convolutional and artificial neural networks (CNNs and ANNs), may play a supportive role and function as catalysts in the management of myopic maculopathy cases in everyday clinical practice. The scientists involved in these surveys successfully arrived at valid conclusions using statistical measurements regarding the effectiveness of various artificial intelligence models in the diagnosis, classification, first screening and follow-up of highly myopic cases. Finally, the studies analyzed before, despite the limitations mentioned, used artificial intelligence techniques that demonstrated sufficient performance and metrics results in diagnosing and monitoring myopic maculopathy cases. However, the need for application of more advanced and diverse imaging techniques (e.g., ultra-wide field fundus MRI and OCT systems) remains imperative to improve image quality and to achieve a more holistic consideration and thorough assessment of this patient population.

References

Asakuma, T., Yasuda M., et al. (2012). Prevalence and Risk Factors for Myopic Retinopathy in a Japanese Population: The Hisayama Study. Ophthalmology 119 (9), 1760-1765. https://doi.org/10.1016/j.ophtha.2012.02.034

Avila, Marcos P. et al. (1984) Natural History of Choroidal Neovascularization in Degenerative Myopia. Ophthalmology, 91 (12), 1573-1581. https://www.aaojournal.org/article/S0161-6420%2884%2934116-1

Chen, Y., Yang, S., Liu, R., et al. (2024). Forecasting myopic maculopathy risk over a decade: Development and validation of an interpretable machine learning algorithm. *Investigative Ophthalmology & Visual Science*, 65(6), 40. https://doi.org/10.1167/iovs.65.6.40.

Curtin, B. J., Karlin, D. B. (1970). Axial length measurements and Fundus Changes of the Myopic Eye. Transactions of the American Ophthalmological Society, 68, 312-334. taos00031-0328.pdf (nih.gov)

Du, R., & Ohno-Matsui, K. (2022). Novel uses and challenges of artificial intelligence in diagnosing and managing eyes with high myopia and pathologic myopia. *Diagnostics*, 12(5), 1210. https://doi.org/10.3390/diagnostics12051210

Du, R., Xie, S., Fang, Y., et al. (2022). Validation of soft labels in developing deep learning algorithms for detecting lesions of myopic maculopathy from optical coherence tomographic images. *Asia-Pacific Journal of Ophthalmology*, 11(3), 227–236. https://doi.org/10.1097/APO.0000000000000466

Du, Y., Chen, Q., Fan, Y., et al. (2021). Automatic identification of myopic maculopathy related imaging features in optic disc region via machine learning methods. *Journal of Translational Medicine*, 19, 167. https://doi.org/10.1186/s12967-021-02818-1

Frisina, R., Gius, I., Palmieri, et al. (2020). Myopic traction maculopathy: Diagnostic and management strategies. Clinical Ophthalmology, 14, 3699–3708. https://doi.org/10.2147/OPTH.S237483

Hayashi, K. et al. (2010). Long- term Pattern of Progression of Myopic Maculopathy: a natural history study. Ophthalmology, 117 (8), 1595-1611. https://www.aaojournal.org/article/S0161-6420%2809%2901291-3

He, X., Ren, P. et al. (2022). Development of a deep learning algorithm for myopic maculopathy classification based on OCT images using transfer learning. Frontiers in Public Health, 10 :1005700. https://doi.org/10.3389/fpubh.2022.1005700

Lewis, J., Garcia, M., et al. (2014) Intact Globe inflation testing of changes in scleral mechanics in myopia and recovery. Experimental Eye Research, 127, 42-48. https://doi.org/10.1016/j.exer.2014.07.004

Li, J., Wang, L., Gao, Y., et al. (2022). Automated detection of myopic maculopathy from color fundus photographs using deep convolutional neural networks. Eye and Vision 9,13. https://doi.org/10.1186/s40662-022-00285-3

Li, Y., Zheng, F., Foo, L. L., et al. (2022). Advances in OCT imaging in myopia and pathologic myopia. Diagnostics, 12(6), 1418. https://doi.org/10.3390/diagnostics12061418

Lu, L., Ren, P., Tang, X., et al. (2021). AI-model for identifying pathologic myopia based on deep learning algorithms of myopic maculopathy classification and “plus” lesion detection in fundus images. *Frontiers in Cell and Developmental Biology*, 9. https://doi.org/10.3389/fcell.2021.719262

Mao, J., Deng, X., Ye, Y., et al. (2023). Morphological characteristics of retinal vessels in eyes with high myopia: Ultra-wide field images analyzed by artificial intelligence using a transfer learning system. *Frontiers in Medicine (Lausanne)*, 9, 956179. https://doi.org/10.3389/fmed.2022.956179

Oh, B.-L., Park, U.C., Kim, B.H., et al. (2022), Role of Ultra-widefield Imaging in the evaluation of Long-term change of highly myopic fundus. Acta Ophthalmol, 100: e977-e985. https://doi.org/10.1111/aos.15009

Ohno Matsui, K. (2014). Proposed Classification of Posterior Staphylomas Based on Analyses of Eye Shape by Three-Dimensional Magnetic Resonance Imaging and Wide-Field Fundus Imaging. Ophthalmology, 121 (9), 1798-1809. https://www.aaojournal.org/article/S0161-6420%2814%2900302-9

Ohno Matsui, K. et al. (2015), International Photographic Classification and Grading System for Myopic Maculopathy. American Journal of Ophthalmology, 159 (5), 877-883. https://www.ajo.com/article/S0002-9394%2815%2900051-3

Page MJ, McKenzie JE, Bossuyt PM, et al. (2021), The PRISMA 2020 statement: An updated guideline for reporting systematic reviews. BMJ. 372:n71. https://doi.org/10.1136/bmj.n71

Panozzo, G., Mercanti, A. et al. (2004). Optical Coherence Tomography Findings in Myopic Traction Maculopathy. Arch Ophthalmology, 122(10), 1455-1460. 10.1001/archopht.122.10.1455

Ruiz-Medrano, J., Montero, J. A., Flores-Moreno, I., et al. (2019). Myopic maculopathy: Current status and proposal for a new classification and grading system (ATN). *Progress in Retinal and Eye Research*, 69, 80–115. https://doi.org/10.1016/j.preteyeres.2018.10.005

Tan, T.-E., et al. (2021). Retinal photograph-based deep learning algorithms for myopia and a blockchain platform to facilitate artificial intelligence medical research: A retrospective multicohort study. The Lancet Digital Health, 3(5), e317–e329. https://doi.org/10.1016/S2589-7500(21)00055-8

Tang, J., Yuan M. et al (2022). An artificial intelligence based automated grading and lesions segmentation system for myopic maculopathy based on color fundus photographs. Transl. Vis. Sci. Technol., 11(6): 16. https://doi.org/10.1167/tvst.11.6.16

Tokoro, T., (1998) Types of Fundus Changes in the Posterior Pole. Atlas of Posterior Fundus Changes in Pathologic Myopia. Springer-Verlag, Tokyo, 5-22. https://doi.org/10.1007/978-4-431-67951-6_3

Wan, C., Fang, J., Hua, et al. (2023). Automated detection of myopic maculopathy using five-category models based on vision Outlooker for visual recognition. *Frontiers in Computational Neuroscience*, 17. https://doi.org/10.3389/fncom.2023.1169464

Ye, X., Wang, J., Chen, Y., et al. (2021). Automatic screening and identifying myopic maculopathy on optical coherence tomography images using deep learning. Translational Vision Science & Technology, 10(13), 10. https://doi.org/10.1167/tvst.10.13.10

Yokoi, T., & Ohno-Matsui, K. (2018). Diagnosis and treatment of myopic maculopathy. *Asia-Pacific Journal of Ophthalmology*, 7(6), 415–421. https://doi.org/10.22608/APO.2018290

Yu, X., Ma, W., Liu, B., et al. (2018). Morphological analysis and quantitative evaluation of myopic maculopathy by three-dimensional magnetic resonance imaging. *Eye*, 32, 782–787. https://doi.org/10.1038/eye.2017.263

Zheng, B., Zhang, M., Zhu, S., et al. (2024). Research on an artificial intelligence-based myopic maculopathy grading method using EfficientNet. *Indian Journal of Ophthalmology*, 72(Suppl 1), S53–S59. https://doi.org/10.4103/ijo.ijo_48_23

Zhu, S., Zhan, H., Wu, M., et al. (2023). Research on classification method of high myopic maculopathy based on retinal fundus images and optimized ALFA-Mix active learning algorithm. *International Journal of Ophthalmology*, 16(7), 995–1004. https://doi.org/10.18240/ijo.2023.07.01

ΥΠΕΥΘΥΝΗ ΔΗΛΩΣΗ

(ΠΕΡΙ ΜΗ ΛΟΓΟΚΛΟΠΗΣ)

Η Μαρία-Βαρβάρα Καπετανάκη του Αργυρίου, με ΑΜ **74507822000014**, γνωρίζοντας τις συνέπειες της λογοκλοπής, δηλώνω υπεύθυνα ότι είμαι η συγγραφέας της παρούσας **Διπλωματικής Εργασίας**, με τίτλο **Artificial Intelligence and Myopic Maculopathy: the Role of Advanced Imaging Techniques in the Diagnosis, Classification and Follow-up of Highly Myopic Cases**, που εκπονήθηκε στα πλαίσια του ΠΜΣ **«Σύγχρονες Προσεγγίσεις στην Παθολογία και Χειρουργική του Αμφιβληστροειδούς»**, της Ιατρικής Σχολής του Ε.Κ.Π.Α.. Η παρούσα διπλωματική εργασία **δεν** αποτελεί αντιγραφή από έντυπες ή ηλεκτρονικές πηγές, μετάφραση από ξενόγλωσσες πηγές και αναπαραγωγή από εργασίες άλλων συγγραφέων, ούτε προέρχεται από ανάθεση σε τρίτους. Αποτελεί προϊόν αυστηρά προσωπικής εργασίας και όλες οι πηγές που χρησιμοποιήθηκαν αναφέρονται σαφώς στη βιβλιογραφία και στο κείμενο, ενώ κάθε εξωτερική βοήθεια, αν υπήρξε, αναγνωρίζεται ρητά σύμφωνα με τους κανόνες της ακαδημαϊκής δεοντολογίας περί αποφυγής της λογοκλοπής.

Μαρία-Βαρβάρα Καπετανάκη

mk